ISSN:1738-6764, eISSN:2093-7504

Visual Taxonomy and Diagnostic Applications of Fluorescence In Situ Hybridization (FISH) Probes in Hematologic, Solid, and Genetic Disorders: A Content-Centric Review

Simon James Fong [1,*], Jinfeng Guo [2], Jiahui Yu [3], Seon-Phil Jeong [4], and Li Bao [5]

[1] Department of Computer and Information Science, University of Macau; ccfong@um.edu.mo
[2] Department of Computer and Information Science, University of Macau; mc46590@um.edu.mo
[3] Department of Computer and Information Science, University of Macau; mc35112@um.edu.mo
[4] Guangdong Provincial Key Laboratory of Interdisciplinary Research and Application for Data Science and Department of Computer Science, Beijing Normal-Hong Kong Baptist University; spjeong@uic.edu.cn
[5] Department of Hematology, Beijing Jishuitan Hospital Affiliated to Capital Medical University, Beijing 100035, China; baoli@jst-hosp.com.cn
* Correspondence

https://doi.org/10.5392/IJoC.2026.22.1.126

Manuscript Received 5 November 2025; Received 11 March 2026; Accepted 21 March 2026

Abstract: *Fluorescence In Situ Hybridization (FISH) is a widely used cytogenetic imaging technique that enables precise visualization of chromosomal abnormalities across a range of clinical contexts. This paper presents a comprehensive visual taxonomy of FISH probe types—deletion/duplication probes (Del/Dup), break-apart probes (BAP), dual-color fusion probes (DC/DF), and centromeric enumeration probes (CEP)—and contextualizes their diagnostic applications across hematologic malignancies, solid tumors, and genetic disorders. By systematically organizing representative FISH imaging patterns and linking them to disease-specific interpretations, this work offers a content-centric reference framework for clinicians, educators, and researchers. The structured atlas not only enhances understanding of probe logic and signal interpretation but also supports the development of digital content systems and clinical decision support tools that integrate cytogenetic imaging with diagnostic workflows.*

Keywords: FISH Imaging; Cytogenetics; Probe Classification; Cancer Diagnostics; Genetic Disorders; Content Taxonomy; Biomedical Visualization; Chromosomal Abnormality Detection; Diagnostic Imaging; Clinical Decision Support

1. Introduction

Fluorescence In Situ Hybridization (FISH) is a cytogenetic imaging technique that enables the visualization of specific DNA sequences on chromosomes using fluorescently labeled probes. Since its development in the 1980s, FISH has become an indispensable tool in clinical diagnostics, particularly for identifying chromosomal abnormalities associated with hematologic malignancies, solid tumors, and genetic disorders [1, 2]. Its ability to detect gene rearrangements, deletions, amplifications, and numerical chromosomal changes in both metaphase and interphase cells has made it a cornerstone of molecular pathology [3]. With the increasing digitization of cytogenetic workflows, FISH has also emerged as a valuable source of structured imaging data that can be analyzed computationally and integrated into bioinformatics pipelines.

The diagnostic utility of FISH is largely determined by the diversity and specificity of its probe designs. Common probe types include deletion/duplication probes (Del/Dup), break-apart probes (BAP), dual-color fusion probes (DC/DF), and centromeric enumeration probes (CEP). Each probe type is tailored to detect distinct genomic events, and their interpretation relies heavily on signal patterns, color combinations, and spatial distribution within the nucleus [4, 5]. Figure 1 provides a conceptual overview of FISH technology and its

diagnostic applications across disease categories. Despite the widespread use of FISH, there remains a lack of unified visual references that systematically organize probe types, signal configurations and their diagnostic manifestations across disease categories.

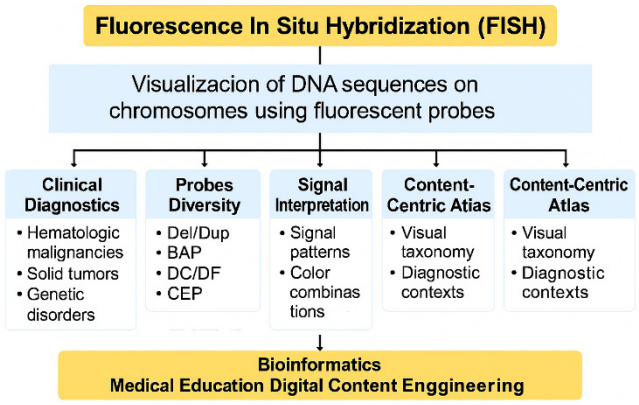

Figure 1. Conceptual overview of Fluorescence In Situ Hybridization (FISH) and its diagnostic landscape. The diagram illustrates the core components of FISH technology - including probe types, signal patterns, and disease applications—and outlines how digitized FISH images can be transformed into structured features for bioinformatics analysis. This includes computational extraction of signal characteristics, integration with genomic datasets, and use in AI-assisted diagnostic pipelines. The figure also motivates the need for a content-centric atlas that standardizes FISH imaging patterns for both clinical interpretation and computational modeling.

The purpose of this study is to address this gap by developing a structured, content-centric atlas that consolidates FISH probe types, canonical signal patterns, and representative diagnostic scenarios across major disease domains. The proposed atlas is designed not only as a visual reference for clinicians and trainees but also as a standardized framework that supports computational analysis, dataset annotation, and integration into bioinformatics and AI-driven diagnostic pipelines. This dual clinical-computational orientation is a defining characteristic of the study, distinguishing it from traditional cytogenetic atlases that focus solely on visual interpretation.

Drawing from published case studies, clinical guidelines, and curated image datasets, we classify and contextualize FISH probe applications in hematologic malignancies (e.g., acute leukemia, chronic myeloid leukemia), solid tumors (e.g., lung, breast, glioma, melanoma), and genetic syndromes (e.g., trisomies, sex chromosome anomalies). The atlas emphasizes interpretation logic, diagnostic thresholds, and probe-specific signal behaviors, providing a coherent taxonomy that links probe architecture to expected visual outcomes.

Beyond its clinical relevance, this work contributes to interdisciplinary domains such as bioinformatics, medical education, and digital content engineering. By organizing FISH content into a visual taxonomy, we aim to support the development of AI-assisted diagnostic tools, enhance educational platforms, and facilitate integration into clinical decision support systems. The atlas serves as both a reference and a foundation for future innovations in cytogenetic imaging and content-driven diagnostics.

2. Methodology

This study adopts a content-centric approach to organize and interpret Fluorescence In Situ Hybridization (FISH) imaging patterns across major disease domains. The methodology involves systematic categorization of probe types, diagnostic contexts, and representative imaging examples drawn from peer-reviewed literature and curated clinical datasets.

To ensure clarity and reproducibility, FISH probes in this study were classified using a multi-criteria framework that reflects both their molecular design and diagnostic function. Classification was based on:

(1) Probe architecture, including whether the probe targets a single locus, flanks a genomic region, or spans two partner genes;

(2) Genomic target characteristics, such as copy-number loci, centromeric repeats, or known fusion breakpoints;

(3) Mechanistic detection strategy, distinguishing probes that detect deletions/duplications, rearrangements, or gene fusions; and

(4) Clinical application domain, including whether the probe is used for aneuploidy screening, fusion detection, or actionable oncogenic alterations.

These criteria align with established cytogenetic practice and allow consistent mapping of probe design to expected signal patterns, interpretation rules, and disease-specific diagnostic thresholds. The resulting four probe classes—Del/Dup, BAP, DC/DF, and CEP—represent the major functional categories used in contemporary clinical FISH assays.

2.1 Probe Type Classification

FISH probes were categorized into four primary types based on their structural design and diagnostic function:

1. Del/Dup (Deletion/Duplication Probes): Target specific loci to detect copy number variations. These probes are paired with internal controls on the same chromosome to confirm loss or gain of signal intensity.
2. BAP (Break-Apart Probes): Designed to flank a gene of interest, these probes detect gene rearrangements or translocations by identifying spatial separation of fluorescent signals.
3. DC/DF (Dual-Color/Dual-Fusion Probes): Used to detect gene fusions by visualizing co-localization of two distinct fluorescent signals, typically red and green, resulting in a yellow fusion signal [6].
4. CEP (Centromeric Enumeration Probes): Target centromeric regions to assess chromosomal number abnormalities, especially in interphase nuclei [7].

Each probe type was mapped to its corresponding signal interpretation logic, including normal vs abnormal configurations, color combinations, and spatial distribution within the nucleus. This classification scheme was selected because it captures the essential mechanistic differences that determine how each probe type generates interpretable fluorescence patterns, thereby enabling systematic comparison across diseases and probe designs.

2.2 Disease Domain Mapping

FISH imaging examples were organized into three major diagnostic domains:

1. Hematologic Malignancies: Including acute promyelocytic leukemia (PML-RARA), Philadelphia chromosome-positive ALL (BCR-ABL1), and CBFB-MYH11 rearrangements in AML [1-3].
2. Solid Tumors: Covering HER2 amplification in breast cancer [5], ALK and ROS1 rearrangements in lung cancer [8], FGFR1 amplification [9], CCNE1 and cyclin D1 amplifications in ovarian cancer, and EWSR1/SS18 rearrangements in sarcomas [6].
3. Genetic Syndromes: Encompassing trisomy 21 (Down syndrome) [10], trisomy 13/18, sex chromosome anomalies (e.g., XXYY, Turner syndrome), and ring chromosome 13 abnormalities.

Each category includes representative FISH images and diagnostic thresholds, with visual examples sourced from published literature and clinical image repositories.

2.3 Source Integration

Image examples and diagnostic criteria were compiled from peer-reviewed case reports, cytogenetic atlases, and journal articles. These sources were selected based on clarity of FISH signal presentation, diversity of probe usage, and relevance to clinical practice. For example, dual-color fusion probes were used to visualize COL1A1-PDGFB fusions in dermatofibrosarcoma protuberans [6], centromeric enumeration probes were applied in prenatal screening for trisomy 21 mosaicism [7], and break-apart probes were used to detect ROS1 rearrangements in lung cancer [8]. FGFR1 amplifications were assessed using copy number thresholds [9], while melanocytic lesion diagnostics incorporated signal imbalance criteria [10].

3. Visual Taxonomy of FISH Probes

Fluorescence In Situ Hybridization (FISH) interpretation rests on recognizing probe design, expected signal geometry, and disease-specific deviations from canonical patterns. This section synthesizes probe mechanics with practical interpretation rules, providing a visual taxonomy that links probe architecture to diagnostic readouts and common pitfalls.

3.1 Probe Classification

The four probe classes reflect distinct molecular strategies for detecting genomic abnormalities: locus-specific copy-number assessment (Del/Dup), breakpoint-oriented rearrangement detection (BAP), partner-specific fusion confirmation (DC/DF), and whole-chromosome enumeration (CEP). This functional separation ensures that signal interpretation rules, thresholds, and diagnostic pitfalls can be described in a standardized and reproducible manner.

Deletion/duplication (Del/Dup) probes target a specific locus and are typically paired with an on-chromosome control probe to distinguish true copy-number changes from technical loss or sectioning artifacts. In a normal cell both target and control signals are present on a homologous chromosome; loss of the target signal relative to the control indicates deletion, while multiple clustered target signals indicate amplification or high-level gain [11]. Del/Dup probes are applied where focal gene dosage alters prognosis or therapy, for example CCNE1 amplification in ovarian carcinoma [12].

Break-apart (BAP) probes flank a gene of interest with two differently colored probes; the diagnostic cue is physical separation of the two fluorochromes in nuclei where the gene has been disrupted or translocated. BAP probes are favored when fusion partners are heterogeneous or unknown, and are widely used for ALK and ROS1 assessments in lung cancer and for detecting cryptic rearrangements in oncology [13, 14].

Dual-color/dual-fusion (DC/DF) probes use two locus-specific probes set to co-localize when a specific gene fusion is present; fused red+green signals produce a yellow (overlap) signal in positive nuclei. DC/DF probes provide high specificity for recurrent fusions with defined partners (e.g., COL1A1-PDGFB in dermatofibrosarcoma protuberans) and are particularly useful when a single, clinically actionable fusion is expected [11], [15].

Centromeric enumeration probes (CEP) target centromeric repeat sequences to report chromosome copy number in interphase nuclei. CEP probes are the standard for rapid aneuploidy screens (e.g., prenatal trisomy panels) and for assessing tumor polyploidy or polysomy where whole-chromosome gains or losses are relevant to diagnosis and prognosis [16], [10].

Figure 2 shows a schematic diagram of the four probe types showing chromosomal probe placement, canonical normal signals, and examples of abnormal patterns for each probe class.

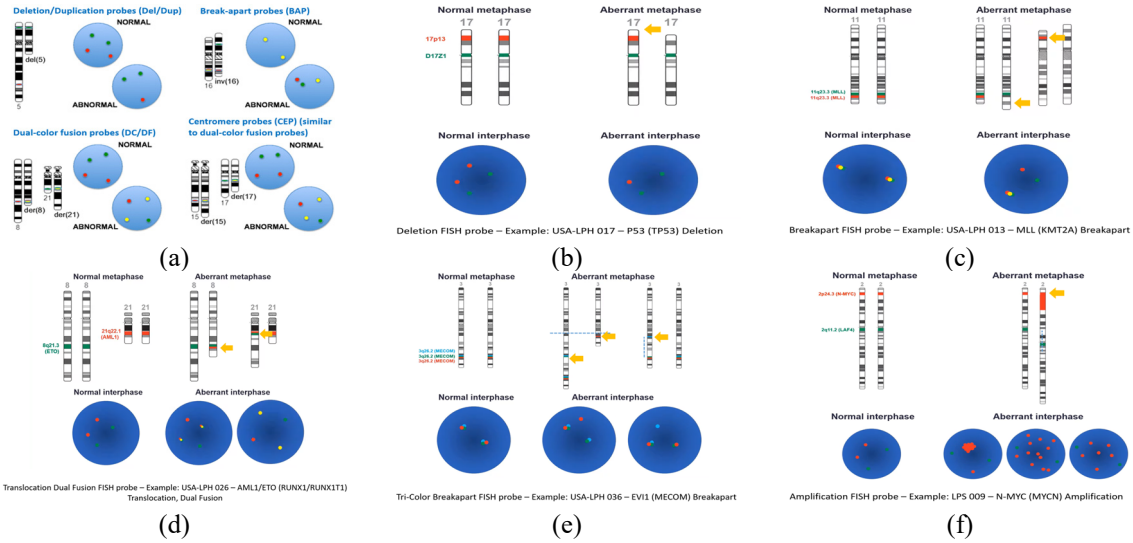

Figure 2. Four types of probes to detect abnormal genes (a) and schematic representation of different FISH probe designs with canonical normal and abnormal signal configurations (b)-(f). Image courtesy of Oxford Gene Technology (OGT) [17]

3.2 Interpretation Logic

Normal versus abnormal signal patterns must be interpreted through defined counting rules, color conventions, and ratio cutoffs. For Del/Dup probes the fundamental rule is concordance between target and control on the unaffected

homolog; deviation in signal count or presence of signal clusters indicates loss or gain respectively, and results are verified across a minimum cell count to avoid false calls from truncation artifacts [11, 12].

Color coding conventions simplify pattern recognition: in break-apart assays a typical design marks the 5' region green and the 3' region red so that a split of red and green beyond a defined distance signals rearrangement; in fusion assays red and green overlap to yield yellow fusion signals when two loci are juxtaposed [13, 14]. Interpreters must account for signal clustering, overlapping nuclei, and sectioning artifacts that can mimic amplification or fusion; these pitfalls are mitigated by using internal controls, examining multiple fields, and applying tumor-specific thresholds.

Diagnostic thresholds vary by application. HER2 amplification is reported using HER2/CEN17 ratios and cluster rules (ratio and percentage-based cutoffs) [18]. FGFR1 amplification in lung cancer is assessed by FGFR1/CEN8 ratio, mean signal counts per nucleus, and the percentage of cells containing high signal clusters, with established cutoffs guiding positive calls [19]. Prenatal and constitutional aneuploidy uses fixed percentage cutoffs from CEP counts to call trisomy or monosomy and requires confirmatory testing for mosaic or borderline results [15], [10]. Figure 3 shows an example of representative signal patterns with annotated interpretation cues and numeric thresholds.

Threshold Setting: Randomly select more than 10 samples of human peripheral blood cells or bone marrow cells, process them according to the sample processing requirements, and prepare negative threshold reference slides. Count 200 cells randomly on each reference slide. Observe the green (BCR) and red (ABL) signal dots within each nucleus.

When the red and green signal dots overlap or their proximity is less than one signal diameter, it is recorded as one fused signal (yellow, F); otherwise it is recorded as one red (R) and one green (G) signal.

- Calculate the total number and percentage of cells showing the 1R1G1F signal type, and statistically calculate the average and standard deviation of the percentage. The negative threshold is set as the average + 3 times the standard deviation, recorded as negative threshold A;
- Calculate the total number and percentage of cells showing other fusion signal types besides 1R1G1F, and statistically calculate the average and standard deviation of the percentage. The negative threshold is set as the average + 3 times the standard deviation, recorded as negative threshold B.

Counting and Interpretation: Count 200 cells. Cells showing the 2 red and 2 green signal types are recorded as FISH negative cells. Cells showing possible n red m green k fusion (n, m, and k are all ≥1, 1 red 1 green 1 fusion is counted separately) signal types are recorded as FISH positive cells.

1. If the proportion of FISH positive cells is greater than the negative threshold, it is judged as FISH positive;
2. If the proportion of FISH positive cells is less than the negative threshold, it is judged as FISH negative;
3. If the proportion of FISH positive cells is equal to the negative threshold, the number of cells counted should be increased or the entire slide should be analyzed (≥500 cells). If it is still less than or equal to the negative threshold, it is considered FISH negative; otherwise, it is considered FISH positive.

Counting and Interpretation Notes:

- a) Unless otherwise specified, only count signals of the form nOmGkF (n≥1, m≥1) during counting;
- b) If there are special circumstances, and a particular signal appears in more than 20% of the cases, it is best to consult literature or relevant materials for verification;
- c) Only count cases where both red and green signals are present. If a large proportion (more than 20%) of cases show no red, no green, or neither, it may be due to sample or experimental conditions. It is best to use a sample with good hybridization signals as a control for comparison.

For example:

Signal type	Cell count
202G	55
101G2F	150
101G1F	5

Result:
101G2F positive cell ratio = 150/(55+150+5) = 71.4%, greater than the threshold value, BCR/ABL fusion positive.

This sample is positive for BCR/ABL gene fusion.
Reference: Negative thresholds for A and B are 12% and 2% respectively.

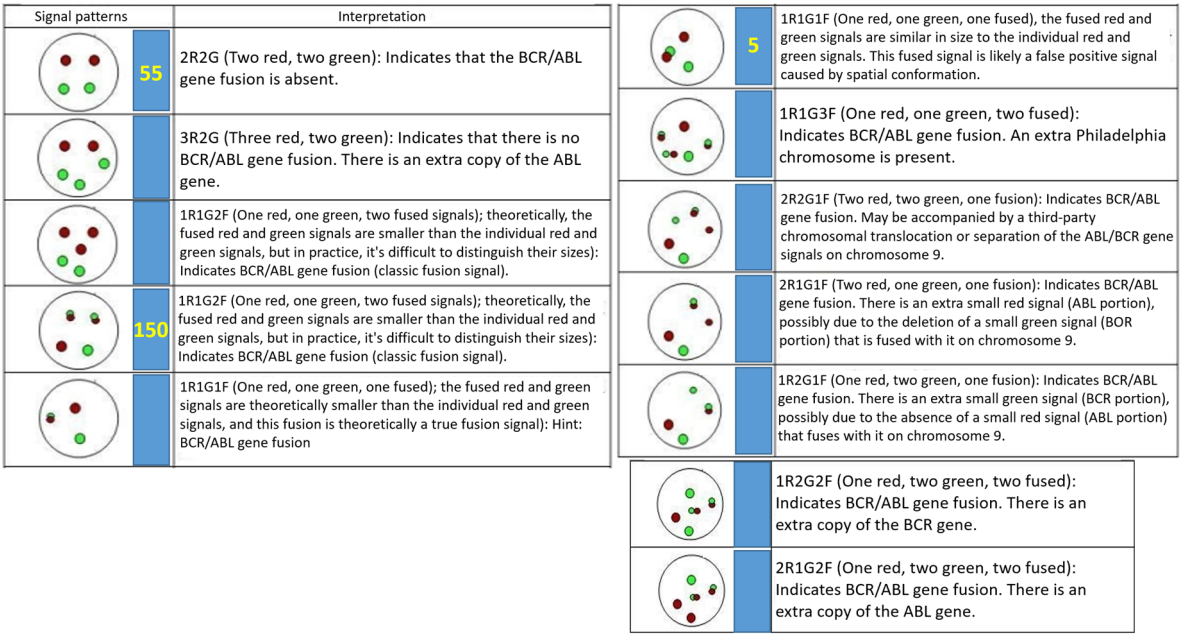

Figure 3. Representative FISH signal example by a real-life leukemia case of BCR-ABL fusion with (Top) the rules and statistics counts in a diagnostic report, and (Bottom) the corresponding annotated interpretation cues and commonly applied diagnostic thresholds. Figure adapted from internal laboratory training materials and standard FISH interpretation guidelines for BCR/ABL fusion detection [20].

4. Applications across Disease Categories

The practical value of the visual taxonomy emerges when probe classes are mapped onto disease contexts. This section describes how each probe type is selected and interpreted across hematologic malignancies, solid tumors, and genetic disorders, illustrated by representative case examples and threshold criteria.

4.1 Hematologic Malignancies

Hematologic diagnostics rely heavily on fusion detection and rearrangement mapping. Dual-color/dual-fusion probes are primary tools for identifying pathognomonic fusions such as PML-RARA in acute promyelocytic leukemia and BCR-ABL1 in Philadelphia chromosome-positive leukemias; fused (yellow) signals in a defined proportion of nuclei support diagnosis and inform therapy [19], [1]. Break-apart probes detect cryptic or variant rearrangements that evade karyotyping, exemplified by CBFB-MYH11 and other cryptic inversions in AML where separation of red and green signals indicates disruption [3].

Del/Dup probes are employed to detect focal copy-number alterations that are clinically relevant for prognosis or therapeutic guidance, such as deletions in tumor suppressor genes or amplifications in oncogenic drivers. These genomic events are confirmed through interphase cell enumeration and comparison with internal control signals [11]. CEP (centromere dual-color) probes are used to assess ploidy changes and whole-chromosome gains, which are often associated with disease progression or resistance to therapy. Their enumeration enables rapid identification of aneuploid cell populations in bone marrow and peripheral blood samples [15].

Figures 4-7 present fluorescence in situ hybridization (FISH) examples from hematologic cases, including:

- Gene fusion (Dual-color fusion probes, DC/DF): DC/DF probes are designed to detect whether two genes or DNA sequences have undergone fusion. A successful fusion event is indicated by a merged red/green fluorescence signal, appearing as yellow.
- Gene deletion or duplication (Deletion/Duplication probes, Del/Dup): These probes are typically paired with contrasting-color control probes on the same chromosome to target specific genes or disease loci. Loss or gain of fluorescent target signals on one chromosome is confirmed by the control probe, which accurately

identifies deletions or duplications. The unaffected homologous chromosome will display both the target and control probes simultaneously.

- Gene rearrangement or translocation (Dual-color break-apart probes, BAP): BAP probes are used to detect translocations or other rearrangements of proto-oncogenes, identifying whether they have fused with other genes or regulatory elements.
- Chromosomal numerical abnormalities (Centromere dual-color probes, CEP): CEP probes are used to count chromosomes within interphase nuclei, enabling detection of numerical abnormalities such as aneuploidy.

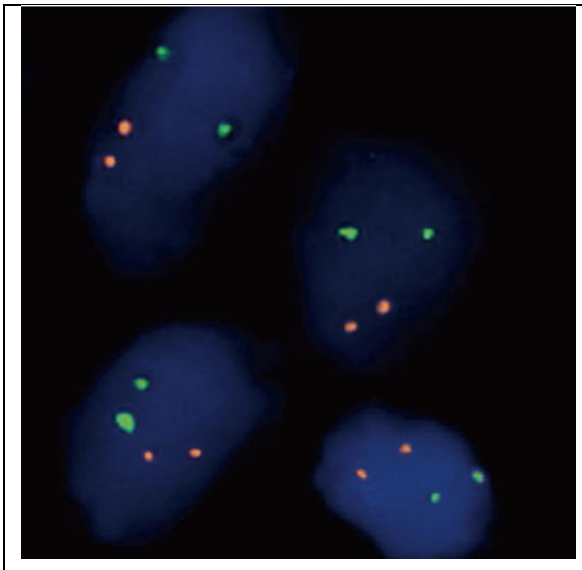

Normal: Two red and two green signals per nucleus, not overlapping. This means no fusion has occurred; the two genes are located on separate chromosomes or loci.

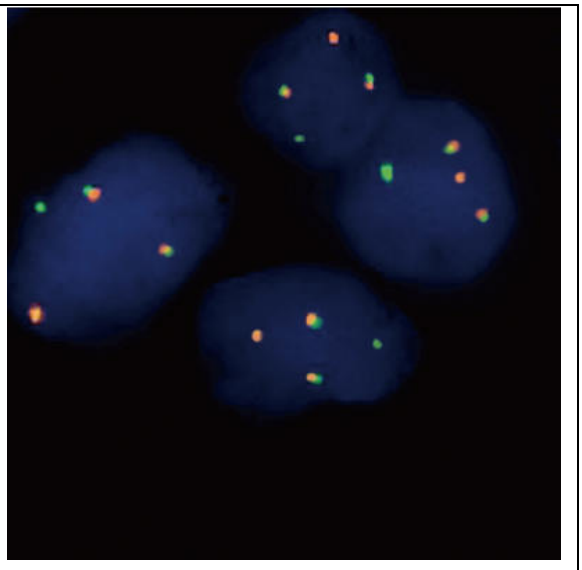

Abnormal: Yellow fusion signals in several nuclei, where red and green overlap. This indicates gene fusion—the two genes are now physically joined due to a translocation. Also there are extra signals, suggesting copy number gain or complex rearrangements.

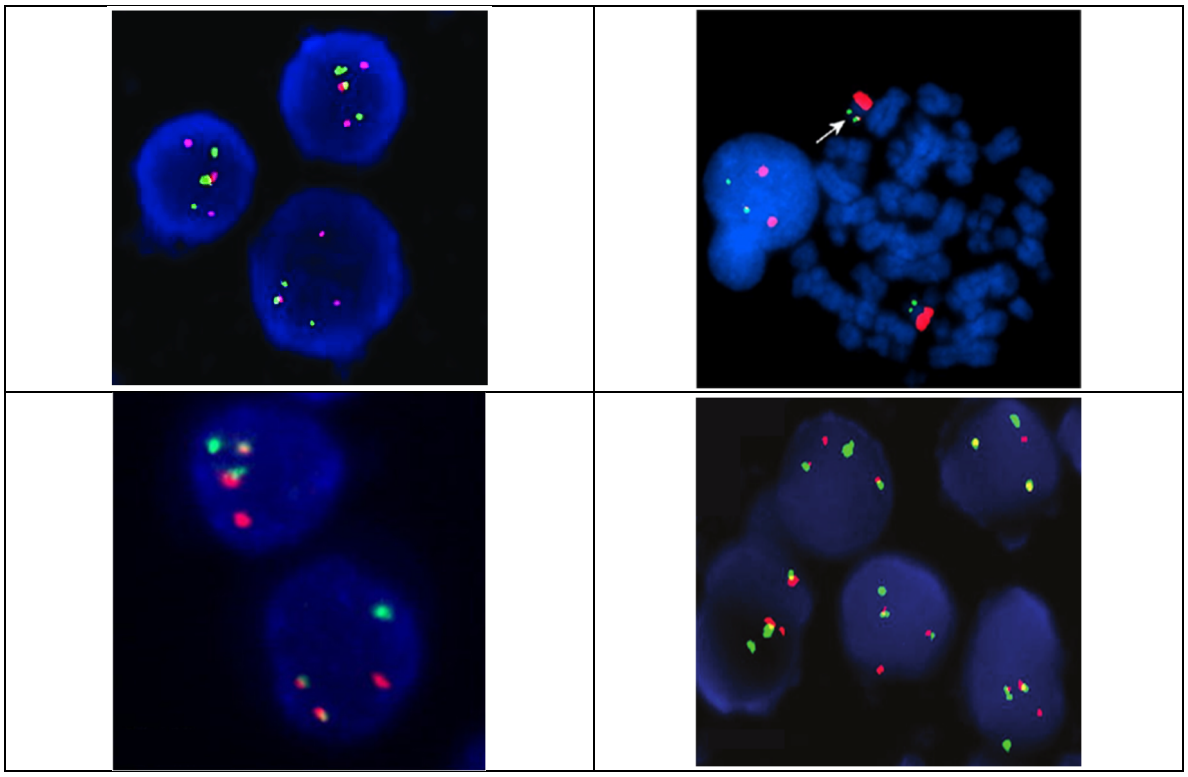

Figure 4. Hematologic malignancy FISH examples: BCR-ABL1 fusion – image courtesy by [1-4], [21].

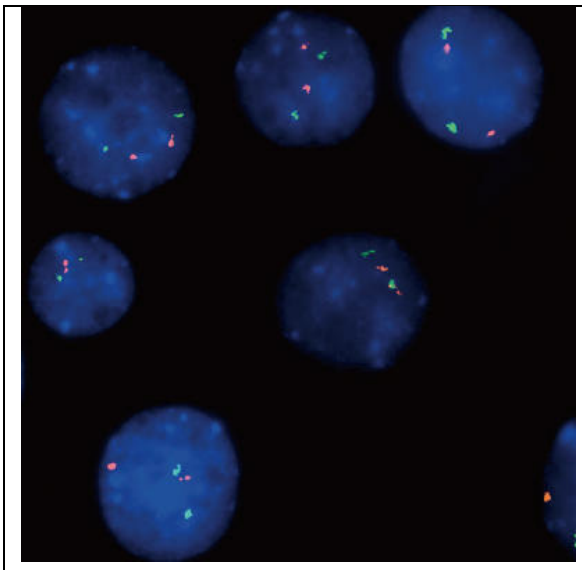

Normal: Each nucleus shows two red and two green signals. This means: Both homologous chromosomes have one copy of the target gene (e.g., red) and one copy of the control region (e.g., green). No deletion or duplication is present. The pairing of red and green signals is balanced.

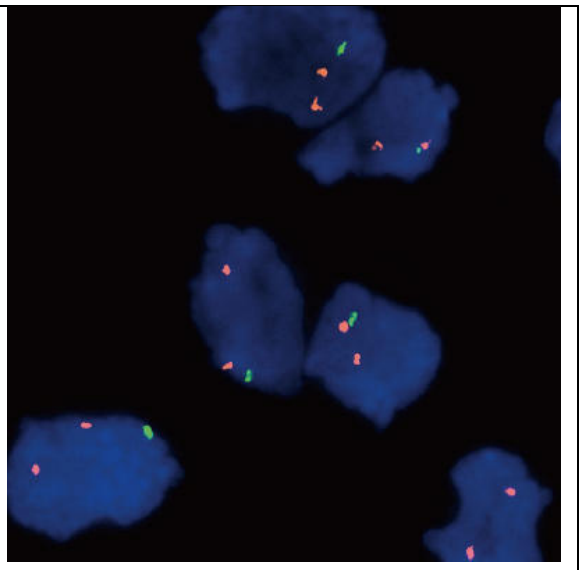

Abnormal: Some nuclei show only one red signal but two green signals. This suggests: Loss (deletion) of the target gene on one chromosome. The control probe (green) confirms the chromosome is present, but the target probe (red) is missing. The other homologous chromosome still shows both signals, confirming the deletion is focal and not a whole-chromosome loss.

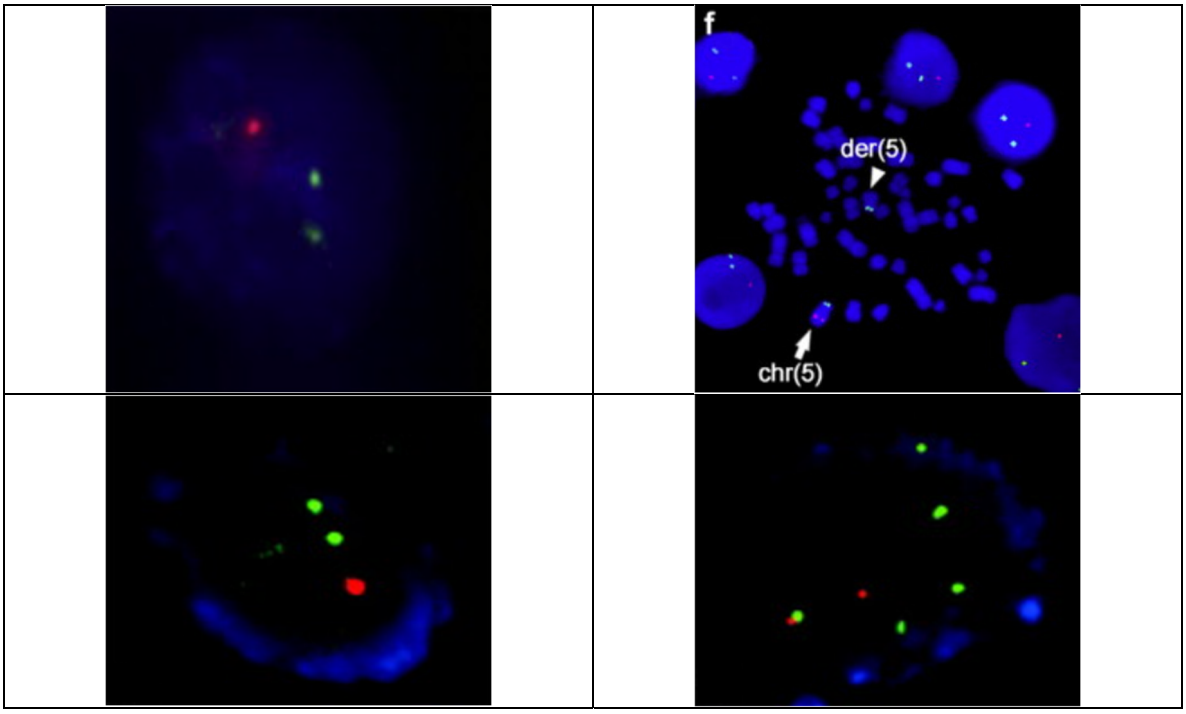

Figure 5. Hematologic malignancy FISH examples: PML-RARA fusion (DC/DF) – image courtesy by [5], [22, 23].

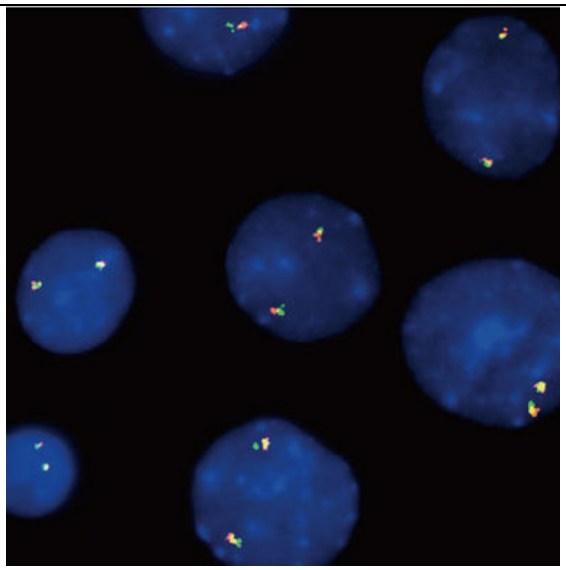

Normal: Yellow fusion signals (overlapping red and green), indicating no rearrangement. This means the gene targeted by the BAP probe is intact.

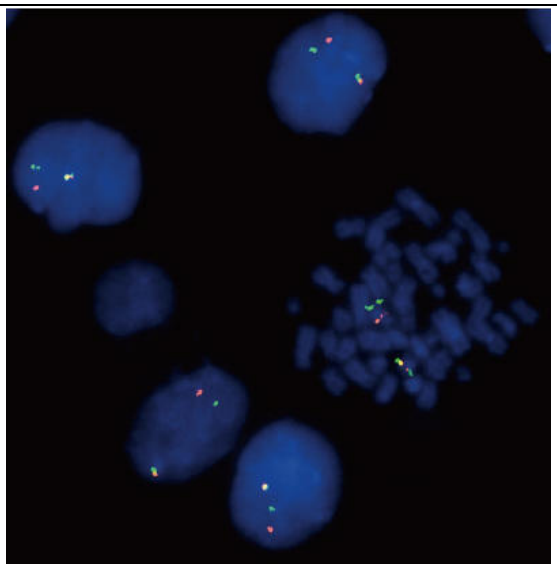

Abnormal: Separated red and green signals in many nuclei. This separation indicates a gene rearrangement or translocation, such as fusion with another gene or regulatory element. The scattered signal pattern may also suggest multiple rearranged copies or amplification.

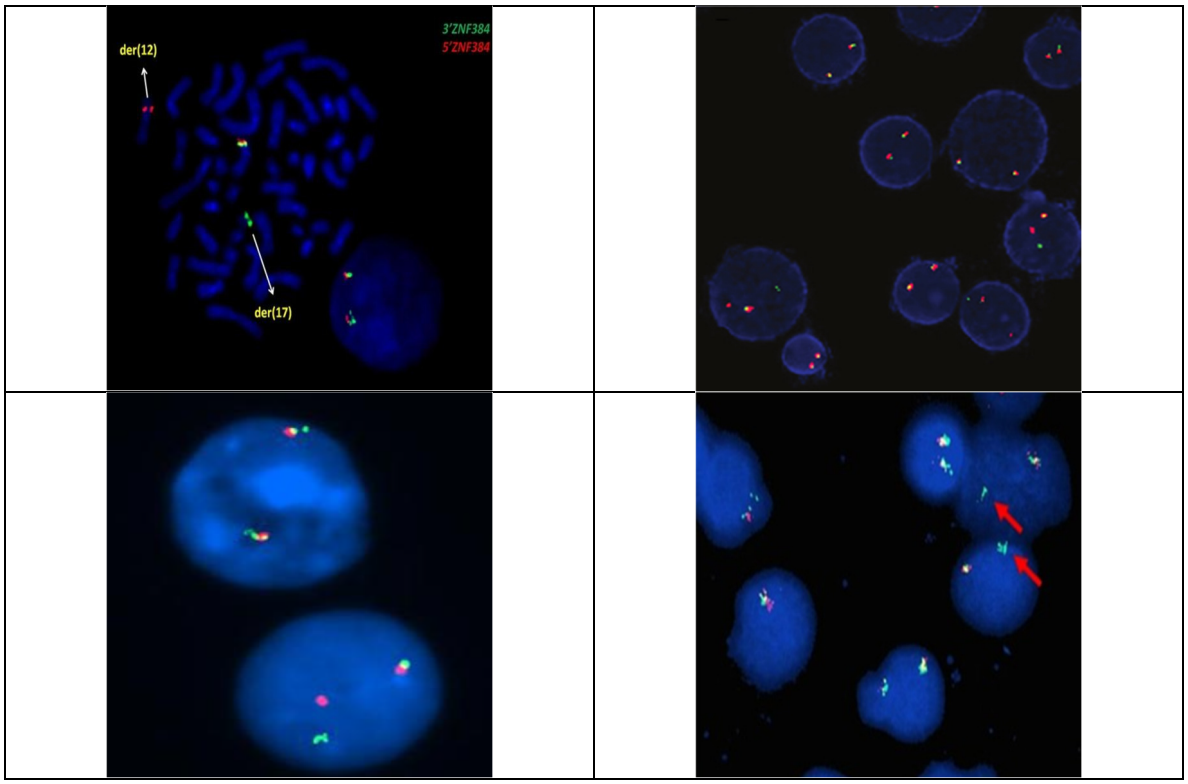

Figure 6. Hematologic malignancy FISH examples: focal deletion detected by Del/Dup probe – image courtesy by [24, 25].

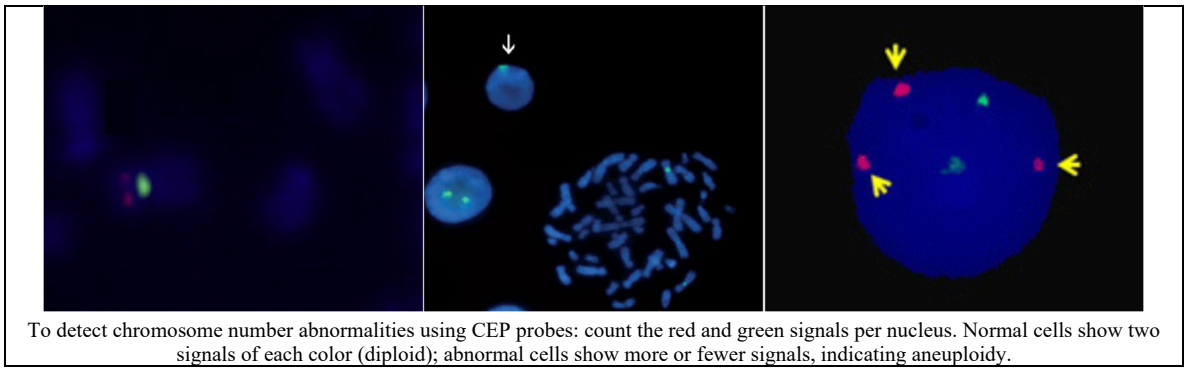

Figure 7. Hematologic malignancy FISH examples: CEP enumeration showing aneuploidy – image courtesy by [26, 27].

4.2 Solid Tumors

FISH plays a pivotal role in identifying actionable genetic alterations in solid tumors. In lung cancer, break-apart and dual-fusion probes detect ALK and ROS1 rearrangements, which predict response to targeted therapies like crizotinib and entrectinib [28, 29] (Figure 8). Breast cancer diagnostics rely on HER2/CEP17 probes to assess HER2 amplification, using HER2/CEP17 ratios, signal clustering, and average copy number to guide anti-HER2 therapy decisions [5], [30-32] (Figure 9). In gliomas, combined locus-specific probes for 1p/19q co-deletion and EGFR amplification help stratify tumor subtypes and inform prognosis and treatment planning [33-35] (Figure 10).

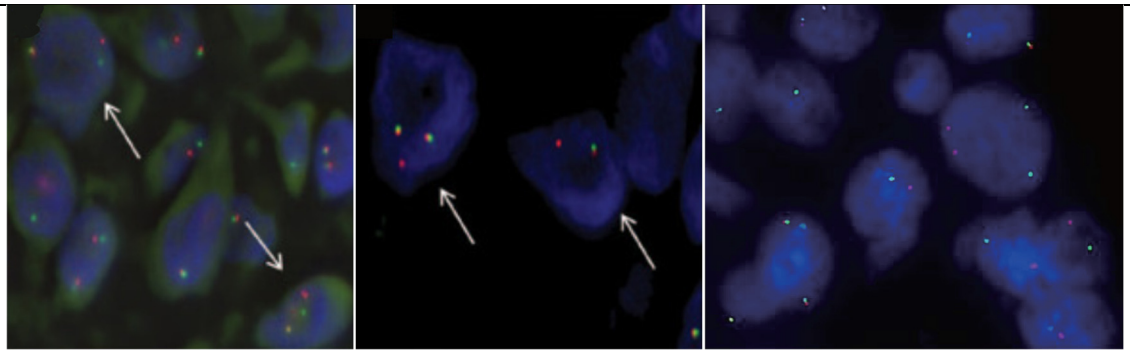

To identify ALK or ROS1 gene rearrangements in lung cancer using FISH: look for whether the red and green signals are fused or separated. Normal cells show fused (yellow) signals; abnormal cells show split red and green signals, indicating gene rearrangement.

Figure 8. Representative solid tumor FISH examples: ALK/ROS1 in lung – image courtesy by [28, 29].

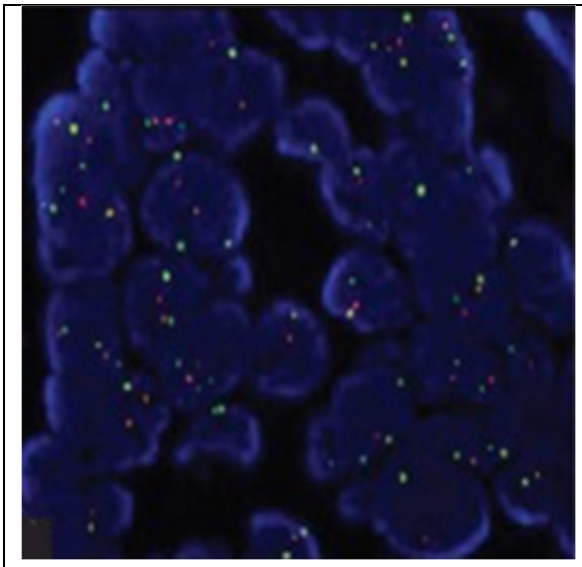

Normal: Each nucleus shows two red HER2 signals and two green CEP17 signals. The HER2/CEP17 ratio is <2.0, and the average HER2 signals per nucleus is <4. This pattern indicates no HER2 amplification (HER2-negative). Patients with this profile are not candidates for HER2-targeted therapy.

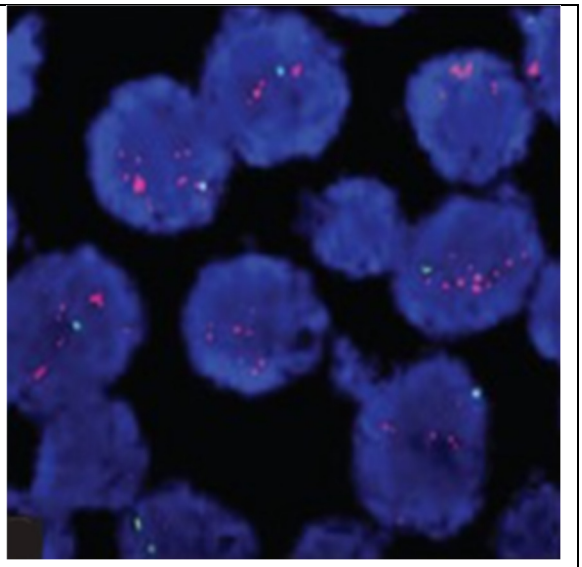

Abnormal HER2 Amplification: Nuclei show multiple red HER2 signals, often exceeding five or more per cell. Green CEP17 signals remain at two, leading to a HER2/CEP17 ratio ≥2.0. This is consistent with HER2 gene amplification, qualifying as HER2-positive breast cancer. These patients are eligible for HER2-targeted treatments.

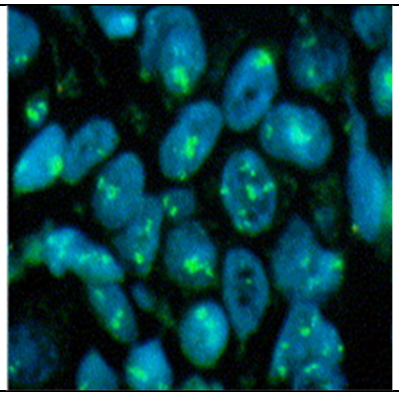

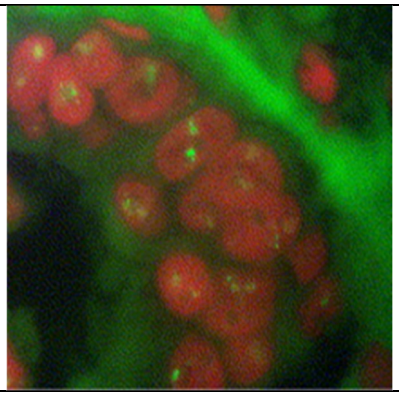

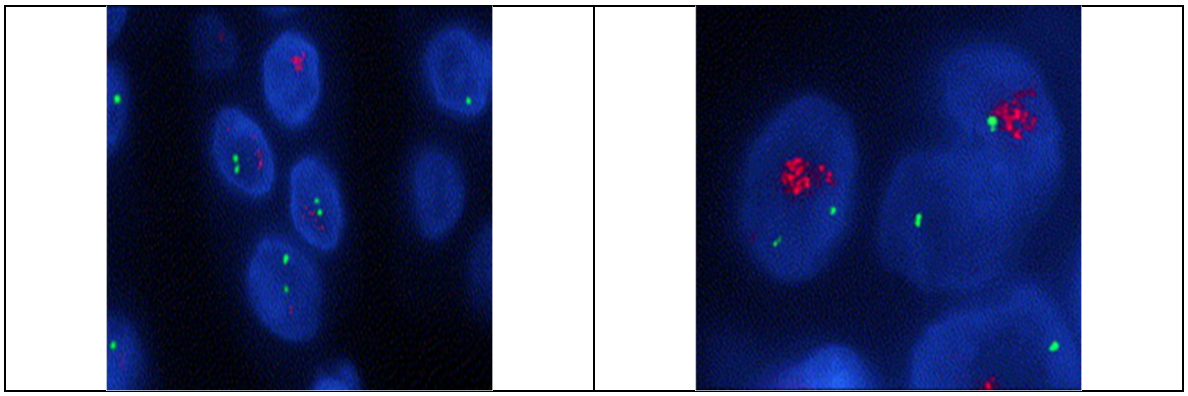

Figure 9. Representative solid tumor FISH examples: HER2 amplification in breast – image courtesy by [5], [30-32].

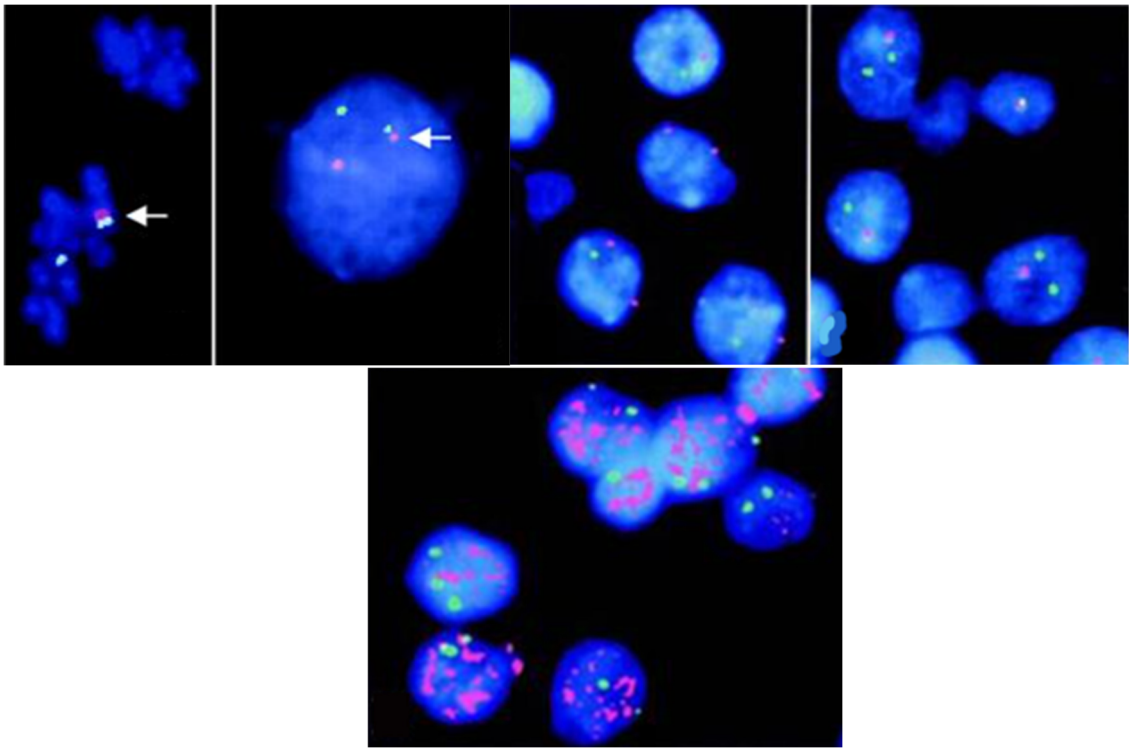

To interpret glioma FISH results for 1p/19q co-deletion, PTEN/DMBT1 co-deletion, and EGFR amplification: look for signal loss (fewer red/green dots) for deletions, and clustered or excessive signals for amplification. Normal cells show balanced, paired signals; abnormal cells show missing or multiplied signals.

Figure 10. Representative solid tumor FISH examples: 1p/19q co-deletion and EGFR amplification in glioma – image courtesy by [33-35].

In ovarian carcinoma, amplification of CCNE1 and cyclin D1 is associated with poor prognosis and chemoresistance. FISH enables quantification of these alterations using locus-specific probes [36, 37] (Figure 11). In Figure 11, normal cells show 2 signals per probe (balanced red/green/blue dots), while abnormal cells show multiple clustered signals—indicating gene amplification (CCNE1, cyclin D1, 20q13) or trisomy (chromosome 8). In high-grade serous ovarian carcinoma, FISH is used to detect gene amplifications and chromosomal number abnormalities that correlate with prognosis and treatment response. The probes used in this context include:

- CCNE1/CEN19p dual-color probe: Detects amplification of CCNE1 (cyclin E1) on chromosome 19q12, with CEN19p as a reference.
- Cyclin D1 DNA probe: Targets CCND1 on chromosome 11q13.

- 20q13 DNA probe: Detects amplification of genes in the 20q13 region, often associated with aggressive tumor behavior.
- Chromosome 8-specific ca-satellite probe: Used to detect trisomy 8, a numerical chromosomal abnormality.

Sarcomas are often defined by characteristic gene rearrangements detectable by break-apart probes. Ewing sarcoma and extraskeletal myxoid chondrosarcoma show EWSR1 and NR4A3 rearrangements [38] (Figure 12), while synovial sarcoma is marked by SS18 translocation [39, 40] (Figure 13). Dermatofibrosarcoma protuberans is diagnosed via COL1A1-PDGFB fusion using dual-fusion probes, which also guide targeted therapy with imatinib [41-44] (Figure 14).

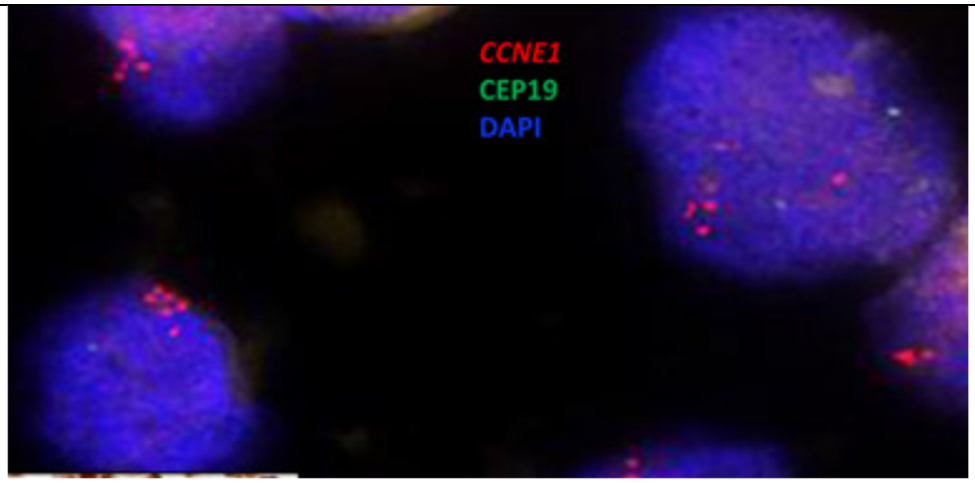

Top image: CCNE1 amplification - you see multiple red signals (CCNE1) per nucleus, often exceeding 6 or forming clusters. Green signals (CEN19p) remain at 2 per nucleus. This indicates high-level CCNE1 amplification, associated with platinum resistance and poor prognosis.

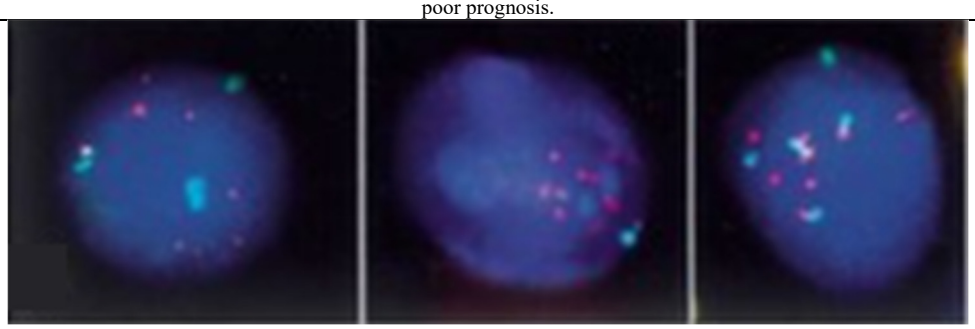

Middle image: 20q13 amplification - Multiple green or aqua signals per nucleus suggest copy number gain in the 20q13 region. This region includes oncogenes like ZNF217, often amplified in ovarian and breast cancers

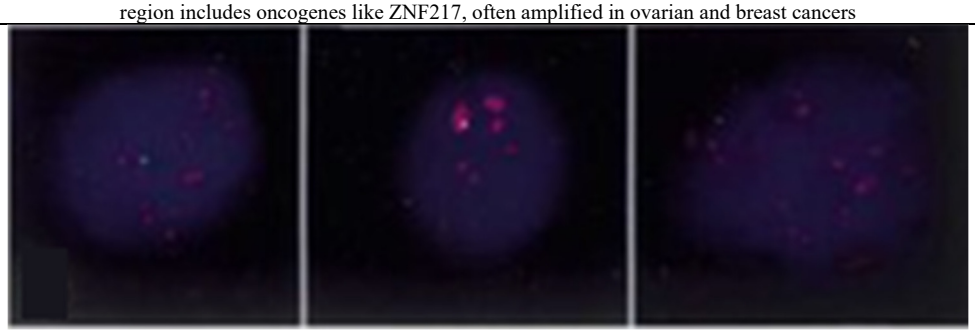

Bottom image: Cyclin D1 amplification - Nuclei show excess red signals for cyclin D1. Normal cells would show 2 signals, but these show ≥6 signals or clusters, indicating amplification. Cyclin D1 overexpression is linked to cell cycle dysregulation and tumor progression.

Figure 11. Representative solid tumor FISH examples: CCNE1/cyclin D1 amplifications in ovarian carcinoma – image courtesy by [36, 37].

EWSR1 and NR4A3 gene rearrangements are detected using break-apart FISH probes: normal cells show fused red/green signals, while abnormal cells show split signals indicating translocation. These rearrangements

are diagnostic for Ewing sarcoma and extraskeletal myxoid chondrosarcoma (EMC). In soft tissue tumors like Ewing sarcoma and extraskeletal myxoid chondrosarcoma (EMC), gene rearrangements involving EWSR1 and NR4A3 are key diagnostic markers. These rearrangements result from chromosomal translocations, most notably:

- t(9;22)(q22;q12) → EWSR1-NR4A3 fusion
- Other variants: TAF15-NR4A3, TCF12-NR4A3, TFG-NR4A3

These fusions drive oncogenic transcription and are detectable by FISH using break-apart probes.

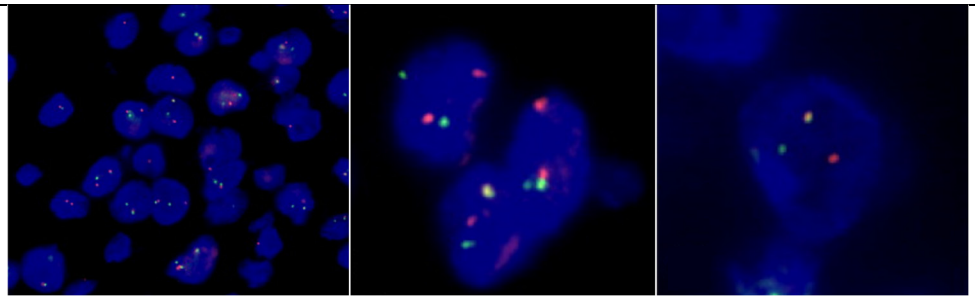

EWSR1 Rearrangement examples: When cells are normal, red and green signals are fused, appearing as yellow. When the genes inside cells are rearranged, red and green signals are split, indicating a break in the EWSR1 locus. This pattern confirms EWSR1 gene rearrangement, seen in ~72% of EMC cases

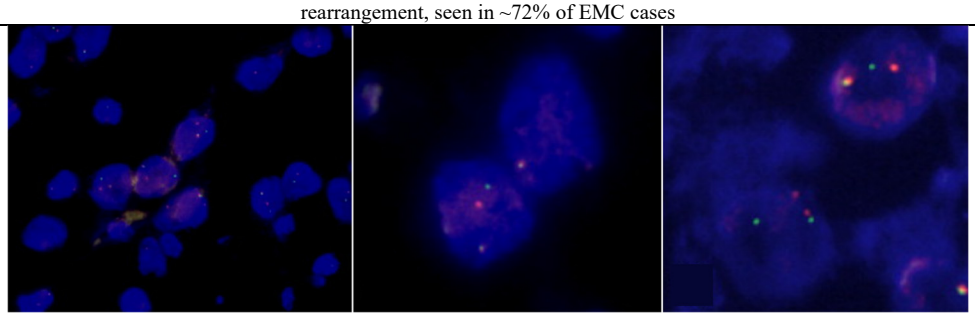

NR4A3 Rearrangement examples: Similar interpretation where split red and green signals indicate NR4A3 rearrangement. NR4A3 fusions are specific to EMC and help distinguish it from other sarcomas. Rearrangement was detected in ~61% of EMC cases, including some EWSR1-negative tumors

Figure 12. Representative solid tumor FISH examples: Ewing sarcoma and extraskeletal myxoid chondrosarcoma show EWSR1 and NR4A3 rearrangements – image courtesy by [38].

To detect SS18 gene rearrangement in synovial sarcoma using FISH: normal cells show fused red and green signals (yellow), while abnormal cells show split red and green signals or isolated red signals—indicating SS18 translocation.

Synovial sarcoma is defined by a specific chromosomal translocation in the example depicted in Figure 13: t(X;18)(p11;q11), resulting in fusion of the SS18 gene (chromosome 18) with SSX1, SSX2, or SSX4 (X chromosome). This fusion drives tumorigenesis and is detectable by SS18 break-apart FISH probes.

- Red probe: telomeric to SS18
- Green probe: centromeric to SS18
- Fused signal (yellow): normal SS18 locus
- Split signals (red and green apart): SS18 rearrangement

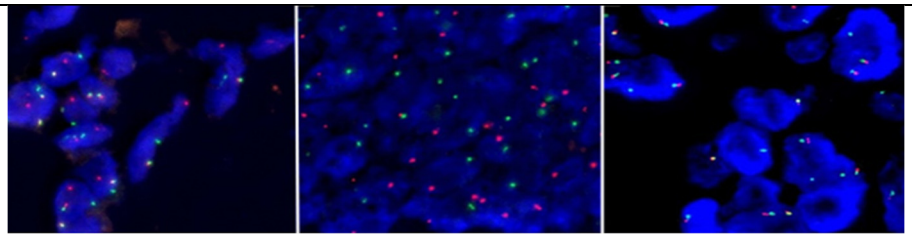

Normal Pattern: Fused red + green signals (yellow dots), that indicates intact SS18 gene, no rearrangement. Seen in non-sarcoma cells or histologic mimics. Abnormal Pattern (Rearranged): Split red and green signals (≥2 signal diameters apart), or isolated red signals without green, that indicates SS18 gene disruption, consistent with synovial sarcoma.s

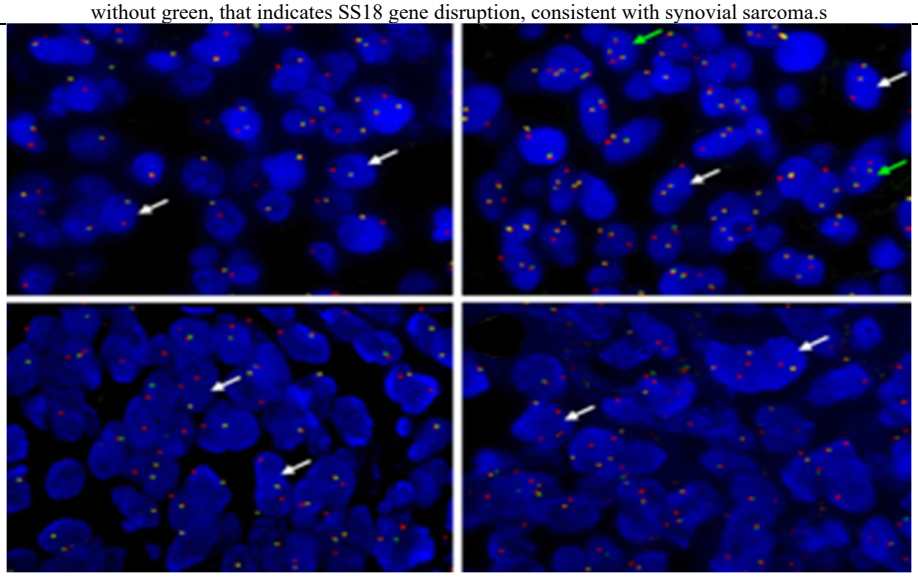

Atypical Patterns (Still Positive): 1F + 1R + 1G: classic break-apart pattern, 1F + 1R, 1F + 1G, 2F + 1R, ≥2F + ≥2R means atypical but often valid. These patterns may reflect unbalanced translocations or complex rearrangements

Figure 13. Representative solid tumor FISH examples: synovial sarcoma is marked by SS18 translocation. – image courtesy by [39, 40].

In dual-color dual-fusion FISH for COL1A1-PDGFB in dermatofibrosarcoma protuberans (DFSP), normal cells show separate red (COL1A1) and green (PDGFB) signals, while abnormal cells show fused yellow signals—indicating gene fusion due to t(17;22)(q22;q13) translocation.

Figure 14 shows an example of COL1A1-PDGFB Fusion in DFSP. Dermatofibrosarcoma protuberans (DFSP) is a low-grade dermal sarcoma characterized by the t(17;22)(q22;q13) translocation, which creates a COL1A1-PDGFB fusion gene. This fusion drives tumor growth via PDGFB receptor activation and is detectable by dual-color dual-fusion FISH probes:

- Red probe: targets COL1A1 on chromosome 17
- Green probe: targets PDGFB on chromosome 22
- Yellow (fused) signal: indicates COL1A1-PDGFB fusion

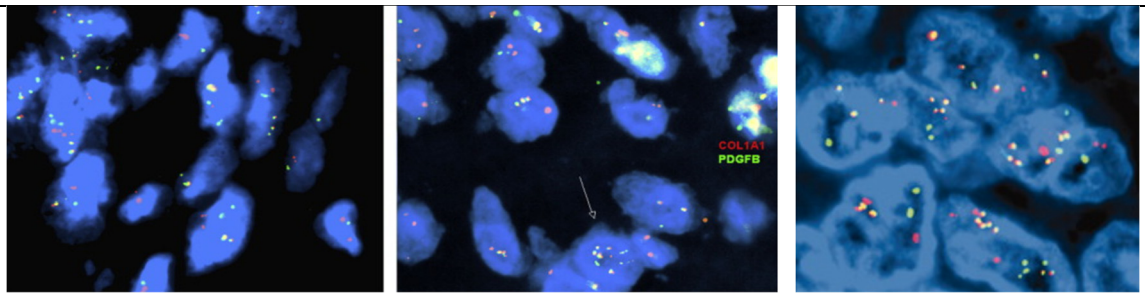

Normal Cells (No Fusion): Show two red signals (COL1A1) and two green signals (PDGFB) per nucleus, signals are spatially separated, indicating no translocation, seen in benign lesions like dermatofibroma or normal tissue. Abnormal Cells (Fusion Positive): show fused yellow signals (overlapping red + green), often accompanied by one red and one green signal (from the non-fused alleles), typical fusion pattern: 1F + 1R + 1G per nucleus, that all indicates COL1A1-PDGFB fusion, diagnostic for DFSP.

Figure 14. Representative solid tumor FISH examples: Dermatofibrosarcoma protuberans (COL1A1-PDGFB): Specific dual-color dual-fusion probe (gene fusion) – image courtesy by [41-44].

In melanoma, chromosomal imbalances on chromosomes 6 and 11 are assessed using a panel of probes targeting RREB1 (6p25), CEP6, MYB (6q23), and CCND1 (11q13). These copy number changes help distinguish malignant melanocytic lesions from benign nevi and correlate with tumor aggressiveness [45-47] (Figure 15). Collectively, these examples underscore the versatility of FISH in solid tumor pathology, where probe design and signal interpretation are tailored to specific genomic alterations, enabling precise molecular classification and personalized treatment strategies.

To interpret melanoma FISH results using RREB1, CEP6, MYB, and CCND1 probes: normal cells show 2 signals per probe, while abnormal cells show increased or decreased signal counts per nucleus. Specific thresholds define malignancy based on signal gain or loss patterns.

Melanoma FISH panels use four probes to detect chromosomal imbalances:

- RREB1 (6p25, red): gain indicates malignancy
- CEP6 (centromere of chromosome 6, aqua): reference for chromosome 6
- MYB (6q23, gold): loss suggests malignancy
- CCND1 (11q13, green): gain indicates proliferation

These probes help distinguish malignant melanomas from benign nevi, especially in histologically ambiguous cases.

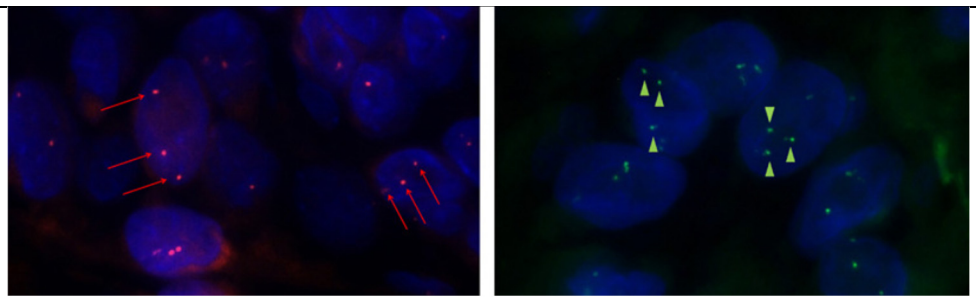

The diagram shows FISH revealed the imbalanced proliferation of cells characteristic of melanoma, especially the increase in red and blue signals. Normal Cells: 2 signals per probe: 2 red (RREB1), 2 aqua (CEP6), 2 gold (MYB), 2 green (CCND1); Balanced signal counts across nuclei that indicates no chromosomal imbalance. Abnormal Cells (Melanoma): CCND1 gain: ≥3 green signals per nucleus in ≥38% of cells, RREB1 gain: ≥3 red signals in ≥29% of cells, RREB1 > CEP6 ratio: more red than aqua signals in ≥55% of cells, and MYB loss: fewer gold signals than aqua in ≥40% of cells.

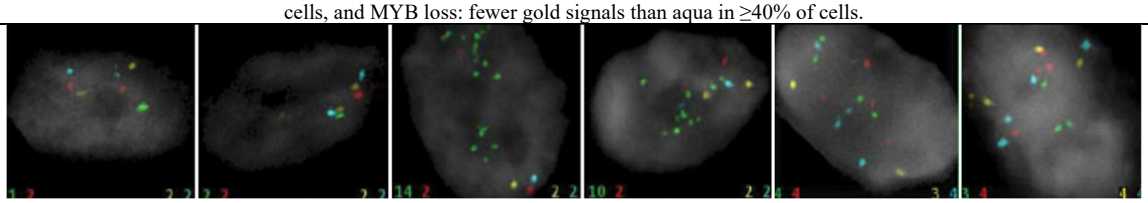

Left image shows excess green signals → CCND1 gain; Middle image shows excess red and green signals → RREB1 and CCND1 gain; Right image patterns meet melanoma thresholds and indicate chromosomal imbalance proliferation P6 ratio: more red than aqua signals in ≥55% of cells, and MYB loss: fewer gold signals than aqua in ≥40% of cells.

Figure 15. Representative solid tumor FISH examples: Melanoma (Chromosome 6): 6p25 (RREB1) probe, CEP6 centromere probe, 6q23 (MYB) probe, and 11q13 (CCND1) probe used to assess melanocytic proliferation – image courtesy by [44-46].

4.3 Genetic Disorders

Interphase FISH using centromere enumeration probes (CEP) remains a cornerstone of rapid aneuploidy screening in both prenatal and constitutional cytogenetics. Standard panels target chromosomes 13, 18, 21, X, and Y, enabling detection of common trisomies (e.g., trisomy 21, 18, 13) and sex chromosome aneuploidies (e.g., Turner syndrome, Klinefelter syndrome). Interpretation follows fixed signal-counting rules, with thresholds for euploid, aneuploid, and mosaic patterns, and confirmatory testing (e.g., karyotyping or microarray) is recommended for borderline or mosaic results [14], [10].

FISH is also applied to segmental deletions, duplications, and ring chromosomes, using locus-specific Del/Dup probes. These allow detection of partial aneuploidies that may be missed by conventional karyotyping. For example, ring chromosome 13 syndrome involves partial or complete loss of the long arm of chromosome 13, often associated with developmental delay, craniofacial anomalies, and organ malformations. Figure 16 illustrates this condition using probes targeting 13q regions [48].

In prenatal workflows, uncultured interphase FISH on amniocytes provides rapid triage for suspected aneuploidies. This is especially useful when ultrasound findings suggest chromosomal abnormalities. Reflex testing with karyotype or chromosomal microarray follows if abnormalities are detected or suspected [10]. Accurate reporting of signal counts, percentage of abnormal cells, and technical limitations is essential to avoid misinterpretation, especially in cases of mosaicism or borderline signal patterns.

Figure 17 shows classic trisomy 21 (Down syndrome), caused by nondisjunction during meiosis, resulting in three copies of chromosome 21 per cell. FISH reveals three red signals for chromosome 21, confirming the diagnosis [7], [49, 50]. Figure 18 depicts a sex chromosome aneuploidy: XXYY syndrome, a rare condition where affected males have two X and two Y chromosomes. FISH shows four signals—two for X and two for Y—compared to the normal XY pattern. This condition is associated with developmental delay, tall stature, and behavioral challenges [51]. Figure 19 illustrates a complex case involving partial monosomy 21 and partial trisomy 1, likely due to an unbalanced translocation. FISH reveals loss of one signal for chromosome 21 and gain of an extra signal for chromosome 1, indicating segmental imbalance [52]. Figure 20 presents trisomy 8, a condition often seen in mosaic form and associated with skeletal anomalies, intellectual disability, and hematologic disorders. FISH using a CEP8 probe shows three signals per nucleus, confirming the gain of chromosome 8 [53].

These examples demonstrate the versatility of FISH in diagnosing both whole-chromosome and segmental abnormalities, with rapid turnaround and high specificity. When integrated with other cytogenetic tools, FISH enhances the accuracy of genetic disorder diagnosis and supports informed clinical decision-making.

In Figure 16, here shows an example of chromosome 13 ring syndrome that is a rare structural abnormality where the long arm of chromosome 13 is partially or completely deleted, and the remaining ends fuse into a ring. This can cause developmental delay, growth restriction, and congenital anomalies. FISH is used to detect deletions at specific loci on chromosome 13:

- LSI 13 (13q14, green): targets the proximal long arm
- D13S327 (13q34, orange): targets the distal long arm

To detect chromosome 13 ring syndrome using FISH: normal cells show two signals for each probe (13q14 and 13q34), while abnormal cells show loss of one or both signals—indicating partial or complete deletion of the long arm of chromosome 13.

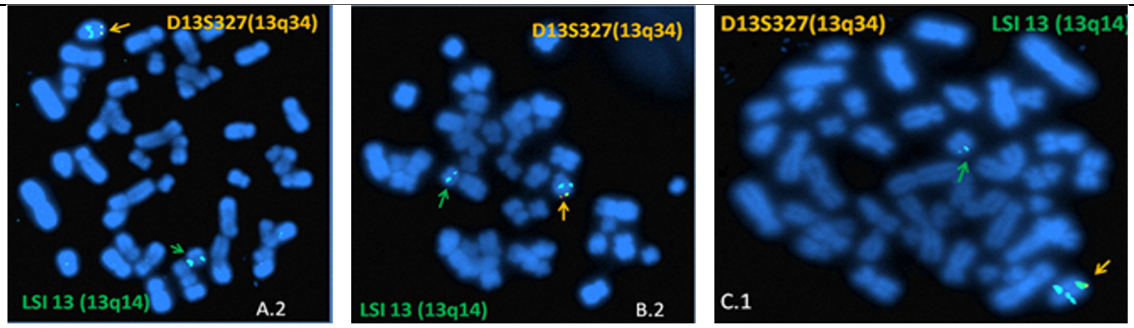

Normal Cells (Panel A.2): Each chromosome 13 shows two green signals (13q14) and two orange signals (13q34); Indicates intact long arm of chromosome 13; No deletion or ring formation. Abnormal Cells (Panels B.2 and C.1): Panel B.2: One chromosome 13 shows loss of orange signal (13q34) while green signal (13q14) remains, it suggests partial deletion of distal 13q; Panel C.1: One chromosome 13 shows loss of both green and orange signals, that indicates complete deletion of 13q, consistent with ring chromosome formation. The arrows highlight chromosomes with missing signals, helping identify the abnormality.

Figure 16. Representative genetic disease FISH example: Ring chromosome 13 syndrome. FISH reveals partial or complete deletion of the long arm of chromosome 13, consistent with ring formation. This abnormality is associated with developmental delay and congenital anomalies. – image courtesy by [48].

Figure 17 shows an example that in FISH for Trisomy 21, normal cells show two red signals for chromosome 21 per nucleus, while abnormal cells show three red signals—indicating an extra copy of chromosome 21, consistent with Down syndrome.

Trisomy 21 (Down syndrome) is a genetic disorder caused by the presence of an extra copy of chromosome 21. It results from nondisjunction during meiosis, leading to three copies of chromosome 21 in affected cells. FISH (Fluorescence In Situ Hybridization) is widely used in prenatal screening and rapid diagnosis, especially on uncultured amniocytes or interphase nuclei.

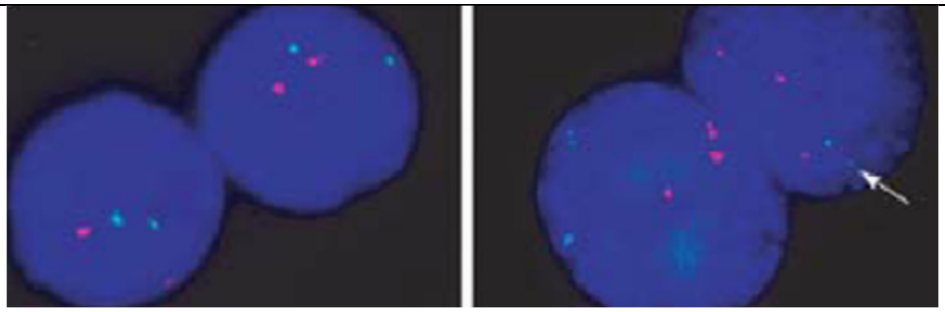

The image shows nuclei stained blue, with red fluorescent signals marking chromosome 21: Left image (Normal) - Each nucleus contains two red signals, representing the two copies of chromosome 21. This is the expected pattern in euploid (normal) cells. Right image (Trisomy 21) - Each nucleus contains three red signals, indicating three copies of chromosome 21. This confirms Trisomy 21, the hallmark of Down syndrome. Arrows in the image point to nuclei with three red signals, helping identify affected cells.

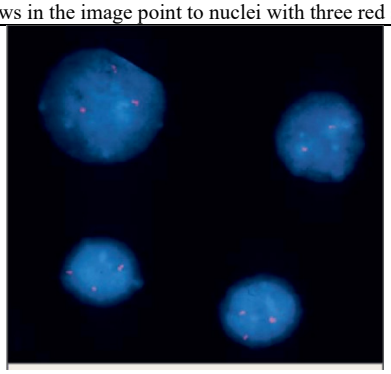

2 red signals means normal (disomic); 3 red signals means Trisomy 21 (down syndrome) and mixed (2 and 3 signals) means mosaicism (requires confirmation). Mosaicism: If some cells show 2 signals and others show 3, this may indicate mosaic Trisomy 21, which can be confirmed by repeat FISH or karyotyping.

Figure 17. Representative genetic disease FISH example: Trisomy 21 (Down syndrome). FISH shows three signals for chromosome 21 per nucleus, indicating nondisjunction and an extra copy of chromosome 21. – image courtesy by [7], [49, 50].

In FISH for sex chromosome analysis, normal male cells show one green signal (X) and one red signal (Y); XXYY cells show two green (X) and two red (Y) signals per nucleus—indicating a sex chromosome aneuploidy.

XXYY syndrome is a rare sex chromosome aneuploidy where males have two X chromosomes and two Y chromosomes instead of the typical XY. It is associated with developmental delays, learning difficulties, tall stature, and sometimes infertility. FISH is used to detect this abnormality by counting fluorescent signals for the X and Y chromosomes in interphase nuclei.

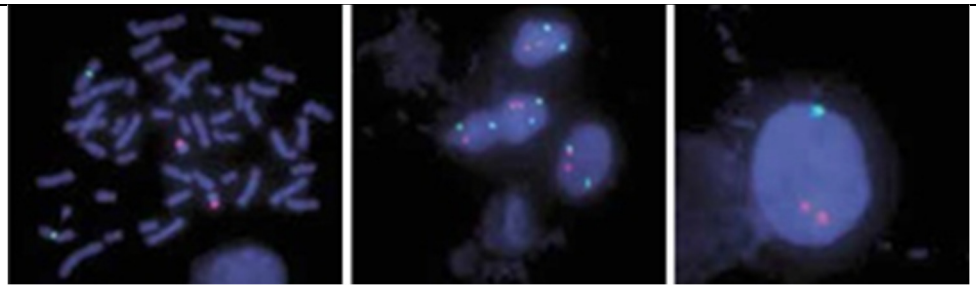

FISH probes typically use: Green signals for the X chromosome, Red signals for the Y chromosome. Normal Male (XY): 1 green (X) + 1 red (Y) signal per nucleus, that indicates a typical male karyotype. XXYY Syndrome: 2 green (X) + 2 red (Y) signals per nucleus that indicates extra copies of both sex chromosomes.

Figure 18. Representative genetic disease FISH example: Sex chromosome aneuploidy – XXYY syndrome. FISH demonstrates two X and two Y signals per nucleus, confirming the presence of four sex chromosomes instead of the normal XY complement. – image courtesy by [51].

In FISH for partial monosomy 21 and partial trisomy 1, abnormal cells show loss of signals for chromosome 21 probes and gain of signals for chromosome 1 probes—indicating segmental imbalance due to an unbalanced translocation.

This condition arises from an unbalanced chromosomal translocation, where part of chromosome 21 is deleted (monosomy) and part of chromosome 1 is duplicated (trisomy). It can occur in embryos or patients with developmental disorders and is detectable using locus-specific FISH probes targeting regions on chromosomes 1 and 21.

The example in Figure 19 shows metaphase chromosomes stained with DAPI (blue), with green and red fluorescent signals marking specific loci:

- Chromosome 21 probe: typically red
- Chromosome 1 probe: typically green

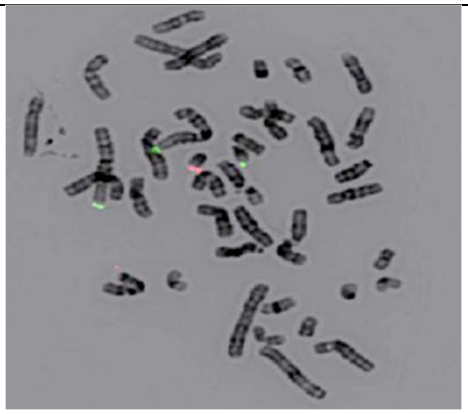

Normal Cells: Show two red signals for chromosome 21 and two green signals for chromosome 1 that indicates normal diploid copy number. Abnormal Cells: Loss of one red signal → partial monosomy 21; Gain of one or more green signals → partial trisomy 1.

These patterns suggest an unbalanced translocation, where part of chromosome 21 is missing and replaced by duplicated material from chromosome 1

Figure 19. Representative genetic disease FISH example: Partial monosomy 21 and partial trisomy 1. FISH reveals loss of one signal for chromosome 21 and gain of an extra signal for chromosome 1, suggesting an unbalanced translocation or complex chromosomal rearrangement. – image courtesy by [52].

Trisomy 8 is diagnosed by FISH when cells show three signals for chromosome 8 per nucleus instead of the normal two—indicating an extra copy of chromosome 8, commonly seen in myelodysplastic syndromes (MDS).

Trisomy 8 is a chromosomal abnormality where cells carry three copies of chromosome 8. It is one of the most frequent cytogenetic findings in myelodysplastic syndromes (MDS) and can be found in both bone marrow and peripheral blood cells. It may occur as a primary abnormality or as part of a complex karyotype [53].

In the example shown in Figure 20, FISH uses a centromeric probe for chromosome 8, typically labeled with a fluorescent dye (often green). The probe binds to the centromere region of chromosome 8 in both metaphase chromosomes and interphase nuclei.

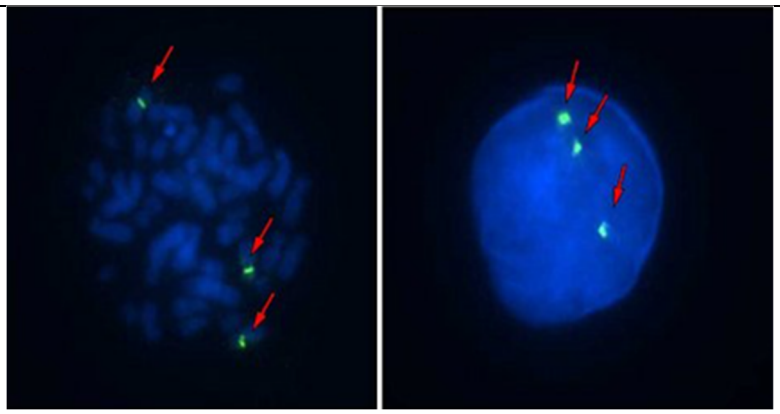

FISH probes typically use: Green signals for the X chromosome, Red signals for the Y chromosome. Normal Male (XY): 1 green (X) + 1 red (Y) signal per nucleus, that indicates a typical male karyotype. XXYY Syndrome: 2 green (X) + 2 red (Y) signals per nucleus that indicates extra copies of both sex chromosomes.

Figure 20. Representative genetic disease FISH example: Trisomy 8. FISH shows three signals for chromosome 8 per nucleus, consistent with full or mosaic trisomy 8, a condition associated with skeletal anomalies and intellectual disability. – image courtesy by [54].

5. Conclusion: Future Prospects and Challenges

The content-centric review of FISH imaging presented in this work consolidates probe design, signal interpretation, and disease-specific applications into a single, practical reference. Unlike existing atlases or narrative reviews, this study introduces a structured, cross-disease visual taxonomy that systematically links Del/Dup, BAP, DC/DF, and CEP probe architectures with their canonical and variant signal patterns. This integrative framework reduces interpretive ambiguity, supports standardized reporting, and provides a reproducible scaffold for training, quality assurance, and computational annotation—features not offered by traditional cytogenetic resources.

The originality of this work lies in its dual clinical–computational orientation. By organizing FISH content into a machine-interpretable structure, the atlas is designed not only for human interpretation but also to enable downstream applications in bioinformatics, AI-assisted diagnostics, and digital content engineering. This positions the atlas as a bridge between classical cytogenetics and emerging computational pathology workflows, addressing a gap in current literature where visual FISH knowledge remains fragmented, unstandardized, and difficult to operationalize for algorithmic use.

Future prospects center on three complementary directions. First, integration with computational tools and machine learning offers scalable, objective interpretation of complex signal patterns, automated quality control, and rapid triage in high-throughput settings. Second, harmonizing visual taxonomies with electronic health records and clinical decision support systems will enable more direct translation of cytogenetic findings into

treatment pathways and outcome tracking. Third, expanded, annotated image repositories and open-access educational resources will accelerate training for pathologists, cytogeneticists, and multidisciplinary teams.

Key challenges remain. Technical variability in specimen preparation, probe performance, and imaging platforms creates interpretive drift that complicates cross-institutional comparability. Biological complexity, including tumor heterogeneity and cryptic rearrangements, requires probe strategies that balance sensitivity and specificity while minimizing false positives from artifacts. Regulatory, interoperability, and data-governance issues must be addressed to safely integrate FISH-derived content into clinical workflows and AI systems.

Recommendations for next steps:

- Standardizing reporting templates and threshold criteria across major FISH applications to reduce interlaboratory variability.
- Developing validated, annotated image datasets and benchmarking challenges to accelerate AI model development and clinical validation.
- Promoting interdisciplinary collaborations between pathology, bioinformatics, and content engineering to operationalize the atlas within clinical decision support and educational platforms.

Collectively, these actions will strengthen the diagnostic utility of FISH, expand its role in precision medicine, and ensure that a structured visual taxonomy remains a practical, evolving resource for clinicians, researchers, and educators.

Acknowledgments: The authors are thankful for the FDCT grants, FDCT-0024/2025/AIJ and FDCT-0019/2025/RIB

Conflicts of Interest: The authors declare no conflicts of interest to report regarding the present study.

References

[1] L. Lv, L. Yang, H. Cui, and T. Ma, "A complex translocation (1;17;15) with spliced short-type PML-RARA fusion transcripts in acute promyelocytic leukemia: A case report," Exp. Ther. Med., vol. 17, no. 2, pp. 1360–1366, 2019, doi: https://doi.org/10.3892/etm.2018.7091.

[2] S. Kohla, S. El Kourashy, Z. Nawaz, R. Youssef, A. Al-Sabbagh, and F. A. Ibrahim, "P190 BCR-ABL1 in a patient with Philadelphia chromosome-positive T-cell acute lymphoblastic leukemia: A rare case report and review of literature," Case Rep. Oncol., vol. 14, no. 2, pp. 1040–1050, 2021, doi: https://doi.org/10.1159/000516270.

[3] H. Zhang, E. M. Sagatys, H. Shao, and K. Liu, "Rare CBFB-MYH11 cryptic rearrangement in acute myeloid leukemia with ins(16)(p13.1q22q22)," Adv. Mod. Oncol. Res., vol. 3, no. 1, pp. 12–14, 2017. [Online] Available: https://api.semanticscholar.org/CorpusID:26991236

[4] W. Chen, J. Yang, and P. Chen, "Cytogenetic characteristics of and prognosis for acute myeloid leukemia in 107 children," Asian Biomed., vol. 15, no. 2, pp. 79–89, 2021, doi: https://doi.org/10.2478/abm-2021-0010.

[5] M. F. Press, D. F. Slamon, K. J. Flom, et al., "HER-2/neu gene amplification characterized by fluorescence in situ hybridization: Poor prognosis in node-negative breast carcinomas," J. Clin. Oncol., vol. 15, no. 8, pp. 2894–2904, 1997, doi: https://doi.org/10.1200/JCO.1997.15.8.2894.

[6] N. Li, T. Zhou, S. Chen, et al., "COL1A1–PDGFB gene fusion in dermatofibrosarcoma protuberans: A useful diagnostic tool and clinicopathological analysis," International Journal of Clinical and Experimental Pathology, vol. 11, no. 8, pp. 4052–4059, 2018.

[7] C. P. Chen, P. T. Wang, S. P. Lin, S. R. Chern, Y. T. Chen, P. S. Wu, Y. L. Kuo, W. L. Chen, and W. Wang, "Interphase FISH on uncultured amniocytes at repeat amniocentesis for rapid diagnosis of true mosaicism involving trisomy 21," Taiwan J. Obstet. Gynecol., vol. 53, no. 1, pp. 120–122, 2014, doi: https://doi.org/10.1016/j.tjog.2013.11.001.

[8] A. Yoshida, T. Kohno, K. Tsuta, S. Wakai, Y. Arai, Y. Shimada, H. Asamura, K. Furuta, T. Shibata, and H. Tsuda, "ROS1-rearranged lung cancer: A clinicopathologic and molecular study of 15 surgical cases," Am. J. Surg. Pathol., vol. 37, no. 4, pp. 554–562, 2013, doi: https://doi.org/10.1097/PAS.0b013e3182758fe6.

[9] A. Dutt, A. H. Ramos, P. S. Hammerman, C. Mermel, J. Cho, T. Sharifnia, et al., "Inhibitor-sensitive FGFR1 amplification in human non-small cell lung cancer," PLoS ONE, vol. 6, no. 6, e20351, 2011, doi: https://doi.org/10.1371/journal.pone.0020351.

[10] J. P. North, J. T. Vetto, R. Murali, K. P. White, C. R. White Jr, and B. C. Bastian, "Assessment of copy number status of chromosomes 6 and 11 by FISH provides independent prognostic information in primary melanoma," Am. J. Surg. Pathol., vol. 35, no. 8, pp. 1146–1150, 2011, doi: https://doi.org/10.1097/PAS.0b013e318222a634.

[11] A. R. Carson, L. Feuk, and S. W. Scherer, "Strategies for the detection of copy number and other structural variants in the human genome," Hum. Genomics, vol. 2, no. 6, pp. 403–410, 2006, doi: https://doi.org/10.1186/1479-7364-2-6-403.

[12] G. Papp, D. Mihály, and Z. Sápi, "Unusual signal patterns of break-apart FISH probes used in the diagnosis of soft tissue sarcomas," Pathol. Oncol. Res., vol. 23, no. 1, pp. 121–129, 2017, doi: https://doi.org/10.1007/s12253-017-0200-z.

[13] K. Takeuchi, N. Okudela, N. Yatabe, et al., "RET, ROS1 and ALK fusions in lung cancer," Nat. Med., vol. 18, no. 3, pp. 378–381, 2012, doi: https://doi.org/10.1038/nm.2644.

[14] P. Martínez, J. H. Landazuri, E. López-Guerrero, et al., "Fluorescence in situ hybridization and immunohistochemistry as diagnostic methods for ALK positive non-small cell lung cancer patients," PLoS ONE, vol. 8, no. 1, e52261, 2013, doi: https://doi.org/10.1371/journal.pone.0052261.

[15] W. Q. Sheng, H. Hashimoto, S. Okamoto, T. Ishida, J. M. Meis-Kindblom, L. G. Kindblom, and M. Hisaoka, "Expression of COL1A1-PDGFB fusion transcripts in superficial adult fibrosarcoma suggests a close relationship to dermatofibrosarcoma protuberans," J. Pathol., vol. 194, no. 1, pp. 88–94, 2001, doi: https://doi.org/10.1002/path.839.

[16] S. G. Vorsanova, et al., "Human interphase chromosomes: a review of available molecular cytogenetic techniques," Mol. Cytogenet., vol. 3, no. 1, article 1, 2010, doi: https://doi.org/10.1186/1755-8166-3-1.

[17] Oxford Gene Technology, Probe map basics. (n.d.). [Online] Available: https://www.ogt.com/us/resources/fish-resources-and-support/introduction-to-fish/probe-map-basics/

[18] T. W. Jacobs, A. M. Gown, H. Yaziji, et al., "Comparison of fluorescence in situ hybridization and immunohistochemistry for the evaluation of HER-2/neu in breast cancer," J. Clin. Oncol., vol. 17, no. 7, pp. 1974–1982, 1999, doi: https://doi.org/10.1200/JCO.1999.17.7.1974.

[19] H. U. Schildhaus, L. C. Heukamp, S. Merkelbach-Bruse, K. Riesner, K. Schmitz, et al., "Definition of a fluorescence in-situ hybridization score identifies high- and low-level FGFR1 amplification types in squamous cell lung cancer," Mod. Pathol., vol. 25, no. 11, pp. 1473–1480, 2012, doi: https://doi.org/10.1038/modpathol.2012.102.

[20] L. G. Shaffer, M. L. Slovak, and L. J. Campbell, (Eds.), ISCN 2009: An international system for human cytogenetic nomenclature, S. Karger, 2009.

[21] B. N. Delikkaya, J. Eberle-Singh, A. B. Morton, J. Z. Gong, and J. Liu, "Uncovering the PML::RARA fusion in cytogenetically cryptic and FISH-negative acute promyelocytic leukemia—A case report and comprehensive literature review," Genes, vol. 16, no. 10, article 1159, 2025, doi: https://doi.org/10.3390/genes16101159.

[22] C. Calderón-Cabrera, I. Montero, R. M. Morales, J. Sánchez, E. Carrillo, T. Caballero-Velázquez, and J. A. Pérez-Simón, "Differential cytogenetic profile in advanced chronic myeloid leukemia with sequential lymphoblastic and myeloblastic blast crisis," Leuk. Res. Rep., vol. 2, no. 2, pp. 79–81, 2013, doi: https://doi.org/10.1016/j.lrr.2013.08.001.

[23] Y. Sun and J. R. Cook, "Fluorescence in situ hybridization for del(5q) in myelodysplasia/acute myeloid leukemia: Comparison of EGR1 vs. CSF1R probes and diagnostic yield over metaphase cytogenetics alone," Leuk. Res., vol. 34, no. 3, pp. 340–343, 2010, doi: https://doi.org/10.1016/j.leukres.2009.05.026.

[24] Y. Wang, Y. Xue, S. Chen, Y. Wu, J. Pan, J. Zhang, and J. Shen, "A novel t(5;11)(q31;p15) involving the NUP98 gene on 11p15 is associated with a loss of the EGR1 gene on 5q31 in a patient with acute myeloid leukemia," Cancer Genet. Cytogenet., vol. 199, no. 1, pp. 9–14, 2010, doi: https://doi.org/10.1016/j.cancergencyto.2010.01.008.

[25] K. A. Abuelgasim, H. Rehan, M. Alsubaie, N. Al Atwi, M. Al Balwi, S. Alshieban, and A. Almughairi, "Coexistence of chronic myeloid leukemia and diffuse large B-cell lymphoma with antecedent chronic lymphocytic leukemia: A case report and review of the literature," J. Med. Case Rep., vol. 12, article 64, 2018, doi: https://doi.org/10.1186/s13256-018-1612-4.

[26] S. Tanizawa, A. R. Koro, L. P. Shi, and M. K. Rodrigues, "Karyotypic and fluorescent in-situ hybridization study of secondary myeloid neoplasms following antineoplastic and/or immunosuppressive therapy," Rev. Bras. Hematol. Hemoter., vol. 33, no. 2, pp. 118–123, 2011.

[27] C. Calderón-Cabrera, I. Montero, R. M. Morales, J. Sánchez, E. Carrillo, T. Caballero-Velázquez, et al., "Differential cytogenetic profile in advanced chronic myeloid leukemia with sequential lymphoblastic and myeloblastic blast crisis," Leuk. Res. Rep., vol. 2, no. 2, pp. 79–81, 2013, doi: https://doi.org/10.1016/j.lrr.2013.08.001.

[28] K. A. Abuelgasim, H. Rehan, M. Alsubaie, N. Al Atwi, M. Al Balwi, S. Alshieban, and A. Almughairi, "Coexistence of chronic myeloid leukemia and diffuse large B-cell lymphoma with antecedent chronic lymphocytic leukemia: A case report and review of the literature," J. Med. Case Rep., vol. 12, article 64, 2018, doi: https://doi.org/10.1186/s13256-018-1612-4.

[29] D. R. Camidge, S. A. Kono, X. Lu, et al., "Anaplastic lymphoma kinase gene rearrangements in non-small cell lung cancer are associated with prolonged progression-free survival on pemetrexed," J. Thorac. Oncol., vol. 6, no. 4, pp. 774–780, 2011, doi: https://doi.org/10.1097/JTO.0b013e31820cf053.

[30] H. R. Kim, S. M. Lim, H. J. Kim, et al., "The frequency and impact of ROS1 rearrangement on clinical outcomes in never smokers with lung adenocarcinoma," Ann. Oncol., vol. 24, no. 9, pp. 2364–2370, 2013, doi: https://doi.org/10.1093/annonc/mdt220.

[31] D. G. Hicks and R. R. Tubbs, "Assessment of the HER2 status in breast cancer by fluorescence in situ hybridization: A technical review with interpretive guidelines," Hum. Pathol., vol. 36, no. 3, pp. 250–261, 2005, doi: https://doi.org/10.1016/j.humpath.2004.11.010.

[32] C. Bozzetti et al., "HER-2/neu amplification detected by fluorescence in situ hybridization in fine needle aspirates from primary breast cancer," Ann. Oncol., vol. 13, no. 9, pp. 1398–1403, 2002. doi: https://doi.org/10.1093/annonc/mdf217.

[33] T. J. Kim et al., "The comparison of automated silver in situ hybridization and fluorescence in situ hybridization for evaluating HER2 gene amplification in breast carcinoma," J. Breast Cancer, vol. 12, no. 4, pp. 295–301, 2009, doi: https://doi.org/10.4048/jbc.2009.12.4.295.

[34] J. W. Bigner, D. D. Friedman, D. W. Miller, et al., "A t(1;19)(q10;p10) mediates the combined deletions of 1p and 19q in human gliomas," Cancer Res., vol. 66, no. 20, pp. 9852–9861, 2006, doi: https://doi.org/10.1158/0008-5472.can-06-1796.

[35] A. Oukhdouch, B. Zinbi, S. Sellami, and H. Rais, "EGFR gene amplification in IDH-wildtype glioblastomas: an integrative bioinformatic and histopathological analysis using immunohistochemistry and fluorescence in situ hybridization," Discov. Oncol., vol. 16, p. 1931, Oct. 21, 2025, doi: https://doi.org/10.1007/s12672-025-03390-6.

[36] C. E. Fuller, R. E. Schmidt, K. A. Roth, P. C. Burger, B. W. Scheithauer, R. Banerjee, K. Trinkaus, R. Lytle, and A. Perry, "Clinical utility of fluorescence in situ hybridization (FISH) in morphologically ambiguous gliomas with hybrid oligodendroglial/astrocytic features," J. Neuropathol. Exp. Neurol., vol. 62, no. 11, pp. 1118–1128, 2003, doi: https://doi.org/10.1093/jnen/62.11.1118.

[37] A. Ayhan, E. Kuhn, R. C. Wu, H. Ogawa, A. Bahadirli-Talbott, T. L. Mao, H. Sugimura, I. M. Shih, and T. L. Wang, "CCNE1 copy-number gain and overexpression identify ovarian clear cell carcinoma with a poor prognosis," Mod. Pathol., vol. 30, no. 2, pp. 297–303, 2017, doi: https://doi.org/10.1038/modpathol.2016.160.

[38] S. A. Ghisai, N. Barin, L. van Hijfte, K. Verhagen, M. de Wit, M. J. van den Bent, Y. Hoogstrate, and P. J. French, "Transcriptomic analysis of EGFR co-expression and activation in glioblastoma reveals associations with its ligands." Neuro-Oncology Advances, vol. 7, no. 1, 2025, doi: https://doi.org/10.1093/noajnl/vdae229.

[39] S. Benini, S. Cocchi, G. Gamberi, G. Magagnoli, D. Vogel, C. Ghinelli, A. Righi, P. Picci, M. Alberghini, and M. Gambarotti, "Diagnostic utility of molecular investigation in extraskeletal myxoid chondrosarcoma," J. Mol. Diagn., vol. 16, no. 3, pp. 314–323, 2014, doi: https://doi.org/10.1016/j.jmoldx.2013.12.002.

[40] T. K. Y. Tay, N. B. Sukma, T. H. Lim, C. H. Kuick, J. Y. Goh, and K. T. E. Chang, "Correlating SS18-SSX immunohistochemistry (IHC) with SS18 fluorescent in situ hybridization (FISH) in synovial sarcomas: A study of 36 cases," Virchows Arch., vol. 479, no. 4, pp. 785–793, 2021, doi: https://doi.org/10.1007/s00428-021-03135-0.

[41] M. F. Amary, F. Berisha, F. del C. Bernardi, A. Herbert, M. James, J. S. Reis-Filho, C. Fisher, A. G. Nicholson, R. Tirabosco, T. C. Diss, and A. M. Flanagan, "Detection of SS18-SSX fusion transcripts in formalin-fixed paraffin-embedded neoplasms: Analysis of conventional RT-PCR, qRT-PCR and dual color FISH as diagnostic tools for synovial sarcoma," Mod. Pathol., vol. 20, no. 4, pp. 482–496, 2007, doi: https://doi.org/10.1038/modpathol.3800761.

[42] H. Noguchi, T. Mitsuhashi, K. Seki, N. Tochigi, M. Tsuji, T. Shimoda, and T. Hasegawa, "Fluorescence in situ hybridization analysis of extraskeletal myxoid chondrosarcomas using EWSR1 and NR4A3 probes," Hum. Pathol., vol. 41, no. 3, pp. 336–342, 2010, doi: https://doi.org/10.1016/j.humpath.2009.04.028.

[43] D. N. Shapiro, M. B. Valentine, S. T. Rowe, A. E. Sinclair, J. E. Sublett, W. M. Roberts, and A. T. Look, "Detection of N-myc gene amplification by fluorescence in situ hybridization: Diagnostic utility for neuroblastoma," Am. J. Pathol., vol. 142, no. 5, pp. 1339–1346, 1993. PMID: 7684192; PMCID: PMC1886925.

[44] M. Tanskanen, T. Jahkola, S. Asko-Seljavaara, J. Jalkanen, and J. Isola, "HER2 oncogene amplification in extramammary Paget's disease," Histopathology, vol. 42, no. 6, pp. 575–579, 2003, doi: https://doi.org/10.1046/j.1365-2559.2003.01648.x.

[45] M. Chen, Y. Li, Z. Ming, A. Biao, and L. X. Zheng, "Comparison of HER2 status by fluorescence in situ hybridisation and immunohistochemistry in gastric cancer," Contemp. Oncol. (Pozn), vol. 18, no. 2, pp. 95–99, 2014, doi: https://doi.org/10.5114/wo.2014.41383.

[46] S. Lodha, S. Saggar, J. T. Celebi, and D. N. Silvers, "Discordance in the histopathologic diagnosis of difficult melanocytic neoplasms in the clinical setting," J. Cutan. Pathol., vol. 35, no. 4, pp. 349–352, 2008, doi: https://doi.org/10.1111/j.1600-0560.2007.00970.x.

[47] E. C. Minca, R. N. Al-Rohil, M. Wang, P. W. Harms, J. S. Ko, A. M. Collie, I. Kovalyshyn, V. G. Prieto, M. T. Tetzlaff, S. D. Billings, and A. A. Andea, "Comparison between melanoma gene expression score and fluorescence in situ hybridization for the classification of melanocytic lesions," Mod. Pathol., vol. 29, no. 8, pp. 832–843, 2016, doi: https://doi.org/10.1038/modpathol.2016.84.

[48] N. Dybdal, G. Leiberman, S. Anderson, B. McCune, A. Bajamonde, R. L. Cohen, R. D. Mass, C. Sanders, and M. F. Press, "Determination of HER2 gene amplification by fluorescence in situ hybridization and concordance with the clinical trials immunohistochemical assay in women with metastatic breast cancer evaluated for treatment with trastuzumab," Breast Cancer Res. Treat., vol. 93, no. 1, pp. 3–11, 2005, doi: https://doi.org/10.1007/s10549-004-6275-8.

[49] J. Wang, S. Zhou, F. He, X. Zhang, J. Lu, J. Zhang, F. Zhang, X. Xu, F. Yang, and F. Xiong, "Familial translocation t(2;4)(q37.3;p16.3), resulting in a partial trisomy of 2q (or 4p) and a partial monosomy of 4p (or 2q), causes dysplasia," Front. Genet., vol. 12, article no. 741607, 2021, doi: https://doi.org/10.3389/fgene.2021.741607.

[50] M. A. Hultén, S. Dhanjal, and B. Pertl, "Rapid and simple prenatal diagnosis of common chromosome disorders: Advantages and disadvantages of the molecular methods FISH and QF-PCR," Reproduction, vol. 126, no. 3, pp. 279–297, 2003, doi: https://doi.org/10.1530/rep.0.1260279.

[51] R. Gupta, V. Patel, S. M. McGinnis, D. Silbersweig, M. B. Miller, M. B. Feany, K. Daffner, and S. A. Gale, "Case study 4: A 68-year-old woman with progressive cognitive decline and anxiety," J. Neuropsychiatry Clin. Neurosci., vol. 35, no. 1, pp. 4-11, 2023, doi: https://doi.org/10.1176/appi.neuropsych.20220151.

[52] J. Blanco, J. Egozcue, and F. Vidal, "Meiotic behaviour of the sex chromosomes in three patients with sex chromosome anomalies (47,XXY, mosaic 46,XY/47,XXY and 47,XYY) assessed by fluorescence in-situ hybridization," Hum. Reprod., vol. 16, no. 5, pp. 887–892, 2001, doi: https://doi.org/10.1093/humrep/16.5.887.

[53] N. Frydman, O. Féraud, C. Bas, M. Amit, R. Frydman, A. Bennaceur-Griscelli, and G. Tachdjian, "Characterization of human PGD blastocysts with unbalanced chromosomal translocations and human embryonic stem cell line derivation," Reprod. Biomed. Online, vol. 19, suppl. 4, p. 4199, 2009. PMID: 20034412.

[54] J. S. Tan, J. A. Gardner, K. A. Devitt, and J. L. Conant, "Myelodysplastic syndrome with excess blasts 2 (MDS-EB-2): A historical overview and review of forthcoming classifications," J. Assoc. Genet. Technol., vol. 49, no. 1, pp. 24–30, 2023. PMID: 36867850.